BJUI
BJU INTERNATIONAL

Usefulness of the 2005 International Society of Urologic Pathology Gleason grading system in prostate biopsy and radical prostatectomy specimens

Hiroji Uemura, Koji Hoshino, Takeshi Sasaki*, Yasuhide Miyoshi†, Hitoshi Ishiguro, Yoshiaki Inayama‡ and Yoshinobu Kubota

*Department of Urology, Yokohama City University Graduate School of Medicine, and Departments of *Pathology, †Urology, Yokohama City University Medical Center, and ‡Department of Pathology, Yokohama City University Hospital, Yokohama, Japan*

Accepted for publication 4 September 2008

Study Type – Prognostic (case series)
Level of Evidence 4

OBJECTIVE

To determine whether the 2005 International Society of Urologic Pathology (ISUP) Gleason Grading Consensus is clinically more useful than the conventional Gleason score (CGS), we compared the CGS and ISUP GS (IGS) of prostate needle biopsy (NB) and radical prostatectomy (RP) specimens, and evaluated the prognostic value of the ISUP GS.

PATIENTS AND METHODS

Of 250 patients undergoing RP, 103 with clinical stage T1–2 N0M0 were enrolled. Pathological tumour grades of NB and RP specimens were classified according to CGS by experienced pathologists in the central pathology department of our hospital, and retrospectively according to IGS by one uropathologist at the central pathology department of another hospital. All patients had RP with no neoadjuvant or adjuvant therapy. We analysed associations of CGS and IGS with biochemical recurrence-free survival (BRFS) after RP.

RESULTS

The concordance rates between NB and RP specimens by CGS and IGS were 64.1% and 69.9%. Under-grading and over-grading rates by CGS and IGS were 28.2% and 7.8% for NB, and 27.2% and 2.9% for RP, respectively. There was a significant difference in the over-grading rate between CGS and IGS ($P = 0.026$). When CGS and IGS of NB and RP specimens were compared, the concordance rates were similar, at 67% and 69.9%. The IGS was higher, by 15.6% in NB and by 20.4% in RP specimens, than CGS. Patients were divided into three groups based on IGS of NB specimens (≤6, 7 and ≥8). These groups differed significantly in BRFS after RP ($P = 0.022$); CGS showed no such association.

CONCLUSIONS

The IGS of NB specimens were significantly associated with BRFS after RP. The ISUP system is thus clinically useful for determining the most appropriate treatments for patients with early-stage prostate cancer.

KEYWORDS

prostate cancer, ISUP Gleason score, needle biopsy, prostatectomy, biochemical failure

INTRODUCTION

Prostate cancer is one of the most common neoplasms in men in the USA and other Western countries. The current widespread use of serum PSA levels and prostate biopsy has increased the detection rate of prostate cancer, resulting in a considerable shift toward earlier stages [1]. Furthermore, it is very important to diagnose prostate cancer at an early stage, when curative treatment is most likely. More patients are now choosing radical prostatectomy (RP), external beam radiotherapy, brachytherapy and active surveillance. In planning these treatments, the primary prognostic factors are the Gleason score (GS) of needle biopsy (NB) specimens, serum PSA level and the DRE findings [2,3].

Among the many factors influencing whether curative treatment or active surveillance is the best option, the GS of NB specimens is more important for patients with early-stage prostate cancer. However, it has been shown that the GS from NB specimens has an inherent sampling error and differs from the GS of RP specimens [4]. The most frequent discordance has been under-grading of the NB GS, although rates of under-grading have gradually decreased since the early 1990s [5]. Some reports have indicated that extended prostate biopsy significantly improves the GS concordance between NB and RP specimens [6,7]. Nevertheless, clinicians should be aware of the GS discrepancy between NB and RP specimens when determining the most appropriate treatments for their patients, especially those with early-stage prostate cancer.

The 2005 International Society of Urologic Pathology (ISUP) Gleason Grading Consensus was proposed to achieve consensus in specific areas of Gleason grading [8]. In particular, the ISUP Gleason grading for NB and RP

TABLE 1 Differences between conventional and 2005 ISUP Gleason scoring

CGS	2005 IGS
A diagnosis of GS <4 possible on NB	GS of NB specimens <4 rarely if ever made.
A partial cribriform pattern, large cribriform, is diagnosed as Gleason pattern 3	Most cribriform patterns would be diagnosed as Gleason pattern 4 while specimens with only rare cribriform lesions would satisfy the diagnostic criteria for cribriform pattern 3.
The same GS are used for NB and RP specimens	Different GS used for NB and RP specimens.
High-grade tumour of small quantity (<5%) on NB should be excluded based on GS (5% threshold rule)	High-grade tumour of any quantity on NB should be included within the GS.
Tumours on NB should be graded by listing the primary and secondary patterns, i.e. excluding tertiary pattern	For the tertiary pattern on NB specimens, both the primary pattern and the highest grade should be recorded.
The GS of RP specimens should be assigned based on the primary and secondary patterns	For RP specimens, the pathologist should assign the GS based on the primary and secondary patterns + a comment on the tertiary pattern
Separate or overall scoring to assess all grades of NB specimens are used	When NB specimens show different grades in separate cores, individual GS should be assigned to these cores (separate scoring).
The grade of the largest portion should be assigned even if the second largest portion is of higher grade	When RP specimens show different grades in separate tumour nodules, a separate GS should be assigned to each of the dominant tumour nodules

TABLE 2 The characteristics of the 103 patients

Variables	Median (95% CI)
Observation period, years	2.1 (1.92–2.40)
Age, years	67 (66–67)
Serum PSA level at RP, ng/mL	9.2 (10.7–14.1)
Clinical stage	
cT1	51 (49.5)
cT2	51 (49.5)
Unknown	1 (1.0)
% positive biopsy cores	25.0 (22.0–28.6)
GS NB by CGS	
≤6	48 (46.6)
7	37 (35.9)
8–10	18 (17.5)
Risk classification by CGS	
Low	34 (33.0)
Intermediate	37 (35.9)
High	32 (31.1)

specimens, the representative points of which are described in below, was altered. There have been no reports evaluating ISUP Gleason grading which include PSA (biochemical) recurrence-free survival (BRFS) after RP. In the present retrospective study, we compared conventional GS (CGS) and ISUP GS (IGS) of NB and RP specimens. Furthermore, we analysed the relationships of CGS and IGS with BRSF after RP, and thereby evaluated the clinical usefulness of IGS specifically in NB specimens.

MATERIALS AND METHODS

In all, 250 patients with prostate cancer diagnosed as clinical stage T1–2 N0M0 received RP at Yokohama City University Hospital from January 1996 to December 2006. Serum PSA levels were determined with a third-generation PSA assay kit. PSA failure after RP was considered to be present when PSA was increased by >0.2 ng/mL. Before RP, all patients had TRUS-guided NB transperineally with 8–12 cores, to confirm the diagnosis of prostate cancer. Clinical stage was determined using MRI, CT and bone scintigraphy.

Of these 250 patients, 103 who did not have neoadjuvant or adjuvant therapies, e.g. hormonal or radiotherapy, were enrolled in the study. Pathological tumour grades of the specimens obtained from NB and RP were classified according to CGS by several pathologists in the central pathology department of Yokohama City Hospital. Later, these NB and RP specimens were classified according to IGS by one uropathologist at the central pathology department of Yokohama City University Medical Center.

In the present study, we used the ISUP Consensus Gleason Grading System [8]. The differences between the ISUP and CGS are shown in Table 1. One pathologist determined the pathology of the dominant tumour nodules, based on rules 7 and 8 in Table 1.

The results were assessed statistically using the Mann–Whitney *U*-test and chi-square test. BRFS was determined by the Kaplan–Meier method, and the significance of differences determined by the log-rank test; in all tests $P < 0.05$ was considered to indicate a statistically significant difference.

RESULTS

The characteristics of the 103 who had not received adjuvant therapies before or after RP are shown in Table 2. Using the risk classification of D'Amico *et al.* [9], the 103 patients were divided into three groups, i.e. 34 low-risk (33%), 37 intermediate-risk (36%) and 32 high-risk (31%).

Correlations between the CGS and IGS of NB and RP specimens are shown in Table 3. The CGS for the NB specimen was concordant

TABLE 3 Correlation of CGS and IGS results between NB and RP specimens

	RP GS, *n*		
NB	≤6	7	8–10
CGS			
NB GS			
≤6	26	20	2
7	3	27	7
8–10	0	5	13
IGS			
NB GS	23	18	1
≤6			
7	3	29	9
8–10	0	0	20

TABLE 4 Comparison of CGS and IGS of NB and RP specimens

	IGS, *n*			
CGS	≤6	7	8–10	Total
NB*				
CGS				
≤6	34	14	0	48
7	8	22	7	37
8–10	0	5	13	18
Total	42	41	20	103
RP†				
CGS				
≤6	18	11	0	29
7	8	34	10	52
8–10	0	2	20	22
Total	26	47	30	103

Mann–Whitney U-test, P = *0.469, †0.329.

with that of the RP specimen in 66 cases (64%). The under-grading rate was 28% (29 cases) and the over-grading rate was 8% (eight cases) for CGS. IGS yielded an under-grading rate of 27% (28 cases), similar to the CGS results. The concordance rate for IGS was slightly higher (70%) than that for CGS, while the over-grading rate was significantly lower with IGS (3%, three cases) than with CGS (8%, eight cases; $P = 0.026$).

Next, we compared the CGS and IGS of NB and RP specimens (Table 4). Although the concordance rates for NB and RP specimens by CGS and IGS were similar, at 67% and 70%, the IGS were higher, by 16% in NB and by 20% in RP specimens, than CGS. However, there were no significant differences between

Risk classification	IGS, *n*			
	Low	Intermediate	High	Total
CGS				
Low	24	10	0	34
Intermediate	5	28	4	37
High	0	4	28	32
Total	29	42	32	103

TABLE 5 Risk classifications with CGS and IGS

Mann–Whitney U-test, P = *0.678.*

	Pathological stage				
NB GS	pT2	pTa	pTb	Total	P chi-square
CGS					0.198
≤6	37	10	1	48	
≥7	26	19	6	51	
IGS					
≤6	30	9	0	39	
≥7	33	20	7	60	

TABLE 6 Comparison of NB GS and pathological staging of RP specimens

FIG. 1. Associations of BRFS according to GS from NB specimens graded by CGS and IGS. (a) In three groups, i.e. CGS ≤6, 7 and ≥8, BFRS was evaluated after RP. (b) In three groups, i.e. IGS ≤6, 7 and ≥8, BFRS was evaluated after RP.

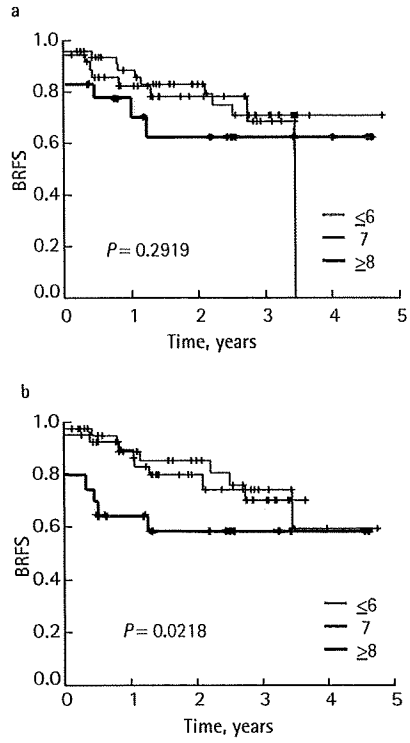

CGS and IGS ($P = 0.469$ for NB and $P = 0.329$ for RP, Mann–Whitney *U*-test). Over-grading rates for NB and RP specimens were 13% and 10% by CGS and IGS, respectively.

Table 5 shows the results grouped by the risk categories of D'Amico *et al.* [9]; 10 (29%) of the 34 categorized as low-risk, based on IGS, were intermediate-risk according to CGS results. Five (14%) and four (11%) of the 37 intermediate-risk, based on CGS, patients were low- and high- risk, respectively, by IGS. However, there were no statistically significant differences in risk classification between CGS and IGS ($P = 0.678$, Mann–Whitney *U*-test).

Clinical staging showed that T1c and T2 each accounted for half the patients; we compared the components of RP pathological staging by CGS and IGS of NB specimens, divided into two groups, GS ≤6 and ≥7. As shown in Table 6, pathological staging by CGS showed predominantly pT2 and pT3a lesions. Among the patients with CGS ≤6 for NB specimens, 37% (pT2) had organ-confined lesions, while 26% of those with CGS ≥7 had organ-confined lesions. However, by contrast with the CGS results, IGS showed an increase in GS ≥7 cases (33%) among those with pT2 tumours, and similar results were obtained for pT3 cases, i.e. 20% in pT3a and 7% in pT3b. However, none of the differences in pathological staging between CGS and IGS were statistically significant ($P = 0.198$, chi-square test).

As shown in Fig. 1A, BRFS in patients with NB specimens classified by CGS did not differ significantly among the three GS groups (≤6, 7 and ≥8). However, when IGS was applied to re-evaluate NB specimens, there was a significant difference in BRFS among these

three groups ($P = 0.022$; Fig. 1B). Likewise, the BRFS in RP specimens, classified by CGS or IGS, were analysed. There were no significant differences in BRFS among the three groups when RP specimens were classified by CGS. However, as when IGS was used to classify NB specimens, the BRFS differed significantly among the three groups ($P = 0.045$; data not shown).

DISCUSSION

The present study showed that nearly a quarter of NB specimens were under-graded in comparison with RP specimens, according to both CGS and IGS evaluations. The GS concordance rates between NB and RP specimens in this study were 64% and 70% by CGS and IGS, respectively, rates similar to those of previous reports (30–74%) [10]. Although we anticipated increased GS up-grading with IGS in both NB and RP specimens, the up-grading rates were only 16% and 20%, respectively. Interestingly, the GS classification of NB by IGS reflected BRFS after RP, although that by CGS did not. Thus, IGS is more reliable for treatment decision-making, especially for early-stage prostate cancer managed with RP, brachytherapy, external beam radiotherapy, hormonal therapy or active surveillance [11].

It was previously reported that the NB pathological findings of focal prostate cancers are not a reliable surrogate indicator, and thus should not influence treatment decisions. One explanation is that prostate cancer is a multifocal disease with satellite tumours [12]. Horinger *et al.* [13] reported that 52 RP specimens had multifocality, showing altogether 196 foci of prostate cancer (the mean number of cancer foci per specimen was 3.76). Other earlier reports also showed that most prostate cancers with high or low tumour volumes were multifocal [14,15]. In these reports, more intriguing results were documented, i.e. very small prostate cancer foci had high GS [13,15]. This might explain why the CGS of NB fails to predict the CGS of RP specimens. CGS does not indicate tertiary cancer lesions or small cancer foci in NB specimens with relatively high Gleason grades, while IGS indicates the primary pattern and the highest grade even in cancer lesions which have small volumes in NB specimens. The present observation that IGS of NB specimens showed significant differences in BRFS after RP suggests the importance of documenting the highest GS in NB.

Khoddami *et al.* [16] reported that primary Gleason pattern 4 had predictive value in patients with Gleason score 7 tumours after RP, meaning that a higher Gleason pattern is important for the prognosis of localized tumours after RP or radiotherapy. From the current results we conclude that the influence of IGS on clinical outcome reflects the grading of NBs based even on minimal findings of high-grade tumour cells. We speculate that Gleason himself might not have recognized the importance of small areas of a third pattern, especially those with the highest grade pattern [17]. However, unlike in the Gleason era, many thin cores from different sites in the prostate can currently be obtained by sextant needle biopsies in patients with early-stage disease, e.g. T1c tumours. Recently, to determine optimum treatments for localized prostate cancer, use of the Partin table, which predicts tumour extension by combining PSA level, clinical stage and GS, has become widespread [18]. Hence, the Partin table might be influenced by IGS, and accumulation of more pathological data on RP specimens will be needed to obtain a new 'Partin table'. Although urologists should prospectively consider differences in NB pathology between CGS or IGS, in practice it would be better to use IGS to obtain of the newest and most reliable nomogram for predicting the outcome of this disease. It is well understood that taking more biopsy cores improves the accuracy of the GS obtained by biopsy in predicting the final GS at RP [9,19]. Furthermore, Antunes *et al.* [20] reported that the percentage of positive biopsy cores reflected the biochemical outcome after RP. In addition, the present results show pathological grading by IGS to reconfirm the accuracy of the biopsy GS before applying treatments for localized prostate cancer.

We showed that 27% more NB than RP specimens were under-graded by IGS, while 28% of NB specimens were under-graded by CGS. The under-grading rate with IGS in our data is consistent with those of earlier reports using CGS [10,21,22]. Previously, GS under-grading of NB specimens was the most prevalent error in comparison with GS grading of RP specimens. Even when the same pathologist assessed both samples, a third of them were still under-graded [22]. Although in the present study the same pathologist evaluated both NB and RP specimens by IGS, the under-grading rate was no less than that by CGS (Table 2). The study of King [23] documented that biases in pathological interpretation and sampling effects contribute to grading discordance. A bias problem in pathological interpretation might be resolved by the widespread use of IGS, especially introducing an assessment of NB specimens.

Fukagai *et al.* [24] indicated that grading errors were most frequent in well-differentiated carcinoma, and that most involved under-grading with poorer NB-RP correlations. They suggested that pathologists tend to under-grade biopsies of moderately differentiated carcinoma as well-differentiated carcinoma. Furthermore, a recent study, examining trends in GS over a period of 15 years, showed that tumours reported as GS ≤6 in NB specimens are prone to be under-graded, while those reported as GS 8–10 are prone to be over-graded [5]. In the light of the change in the GS reporting trend between 1992 and 2006, a progressive increase in Gleason grade 3 and a decrease in Gleason grade 2 were confirmed [25], showing a tendency for an increase in the incidence of moderately differentiated tumours and a decrease in that of well-differentiated tumours. Based on those analyses, the reduction in GS discrepancy between NB and RP specimens would be expected from the redefinition of the Gleason grading system for NB specimens [26,27]. In this respect, the IGS system provides a new definition, described above. The Consensus Conference on Gleason Grading of Prostatic Carcinoma recommended that the GS be the sum of the most common and the highest grade patterns, and that cribriform patterns be diagnosed as Gleason pattern 4 with only rare cribriform lesions satisfying the diagnostic criteria for cribriform pattern 3 [8]. According to the IGS system, under-grading of NB, i.e. GS ≤6, would decrease markedly, while over-grading, i.e. GS >6, would increase.

In conclusion, although the GS under-grading rates in NB and RP specimens did not differ between the CGS and IGS systems, the GS of NB specimens determined by IGS were associated with a significant difference in BRFS after RP, with GS scores similar to those determined using RP specimens. Given that an extended NB scheme and/or the development of a more suitable ultrasound device is expected, the IGS system would

enhance the accuracy of histological assessments of prostate cancer. This will allow physicians caring for patients with prostate cancer to optimize therapies such as RP, brachytherapy, external beam radiotherapy and active surveillance.

ACKNOWLEDGEMENTS

This study was supported by a Grant-in-Aid for Scientific Research (C) from the Ministry of Education, Culture, Science and Technology, a grant for the 2007 Suzuki Foundation, Yamaguchi Endocrine Disease Foundation, the Third-term Cancer Control Strategy Program from the Ministry of Health, Labor and Welfare, and a grant for 2008 Strategic Research Projects (No. K20003 and K20010) of Yokohama City University, Japan.

CONFLICT OF INTEREST

None declared.

REFERENCES

1 **Draisma G, Boer R, Otto SJ *et al.*** Lead times and overdetection due to prostate-specific antigen screening: estimates from the European Randomized Study of Screening for Prostate Cancer. *J Natl Cancer Inst* 2003; **95**: 868–78
2 **D'Amico AV, Whittington R, Malkowicz SB *et al.*** Pretreatment nomogram for prostate-specific antigen recurrence after radical prostatectomy or external-beam radiation therapy for clinically localized prostate cancer. *J Clin Oncol* 1999; **17**: 168–72
3 **Partin AW, Kattan MW, Subong EN *et al.*** Combination of prostate-specific antigen, clinical stage, and Gleason score to predict pathological stage of localized prostate cancer. A multi-institutional update. *JAMA* 1997; **277**: 1445–51
4 **Sved PD, Gomez P, Manoharan M *et al.*** Limitations of biopsy Gleason grade: implications for counseling patients with biopsy Gleason score 6 prostate cancer. *J Urol* 2004; **172**: 98–102
5 **Rajinikanth A, Manoharan M, Soloway CT *et al.*** Trends in Gleason score: concordance between biopsy and prostatectomy over 15 years. *Urology* 2008; **72**: 177–82
6 **Mian BM, Lehr DJ, Moore CK *et al.*** Role of prostate biopsy schemes in accurate prediction of Gleason scores. *Urology* 2006; **67**: 379–83
7 **San Francisco IF, DeWolf WC, Rosen S *et al.*** Extended prostate needle biopsy improves concordance of Gleason grading between prostate needle biopsy and radical prostatectomy. *J Urol* 2003; **169**: 136–40
8 **Epstein JI, Allsbrook WC Jr, Amin MB, Egevad LL.** The 2005 International Society of Urological Pathology (ISUP) Consensus Conference on Gleason Grading of Prostatic Carcinoma. *Am J Surg Pathol* 2005; **29**: 1228–42
9 **D'Amico AV, Whittington R, Malkowicz SB *et al.*** Calculated prostate cancer volume greater than 4.0 cm3 identifies patients with localized prostate cancer who have a poor prognosis following radical prostatectomy or external-beam radiation therapy. *J Clin Oncol* 1998; **16**: 3094–100
10 **Koksal IT, Ozcan F, Kadioglu TC *et al.*** Discrepancy between Gleason scores of biopsy and radical prostatectomy specimens. *Eur Urol* 2000; **37**: 670–4
11 **Hardie C, Parker C, Norman A *et al.*** Early outcomes of active surveillance for localized prostate cancer. *BJU Int* 2005; **95**: 956–60
12 **Donohue RE, Miller GJ.** Adenocarcinoma of the prostate: biopsy to whole mount. The Denver VA experience. *Urol Clin North Am* 1991; **18**: 449–52
13 **Horninger W, Berger AP, Rogatsch H *et al.*** Characteristics of prostate cancers detected at low PSA levels. *Prostate* 2004; **58**: 232–7
14 **Djavan B, Mazal P, Zlotta A *et al.*** Pathological features of prostate cancer detected on initial and repeat prostate biopsy: results of the prospective European Prostate Cancer Detection study. *Prostate* 2001; **47**: 111–7
15 **Djavan B, Susani M, Bursa B *et al.*** Predictability and significance of multifocal prostate cancer in the radical prostatectomy specimen. *Tech Urol* 1999; **5**: 139–42
16 **Khoddami SM, Shariat SF, Lotan Y *et al.*** Predictive value of primary Gleason pattern 4 in patients with Gleason score 7 tumours treated with radical prostatectomy. *BJU Int* 2004; **94**: 42–6
17 **Gleason DF.** Histological grading and clinical staging of prostatic carcinoma. In Tannenbaum M ed., *Urologic Pathology: the Prostate*. Philadelphia: Lea and Feibiger, 1977: 171–98
18 **Richstone L, Bianco FJ, Shah HH *et al.*** Radical prostatectomy in men aged > or = 70 years: effect of age on upgrading, upstaging, and the accuracy of a preoperative nomogram. *BJU Int* 2008; **101**: 541–6
19 **Coogan CL, Latchamsetty KC, Greenfield J *et al.*** Increasing the number of biopsy cores improves the concordance of biopsy Gleason score to prostatectomy Gleason score. *BJU Int* 2005; **96**: 324–7
20 **Antunes AA, Srougi M, Dall'Oglio MF *et al.*** The percentage of positive biopsy cores as a predictor of disease recurrence in patients with prostate cancer treated with radical prostatectomy. *BJU Int* 2005; **96**: 1258–63
21 **Divrik RT, Eroglu A, Sahin A *et al.*** Increasing the number of biopsies increases the concordance of Gleason scores of needle biopsies and prostatectomy specimens. *Urol Oncol* 2007; **25**: 376–82
22 **Lattouf JB, Saad F.** Gleason score on biopsy: is it reliable for predicting the final grade on pathology? *BJU Int* 2002; **90**: 694–8
23 **King CR.** Patterns of prostate cancer biopsy grading: trends and clinical implications. *Int J Cancer* 2000; **90**: 305–11
24 **Fukagai T, Namiki T, Namiki H *et al.*** Discrepancies between Gleason scores of needle biopsy and radical prostatectomy specimens. *Pathol Int* 2001; **51**: 364–70
25 **Sengupta S, Slezak JM, Blute ML *et al.*** Trends in distribution and prognostic significance of Gleason grades on radical retropubic prostatectomy specimens between 1989 and 2001. *Cancer* 2006; **106**: 2630–5
26 **Gleason DF.** Histologic grading of prostate cancer: a perspective. *Hum Pathol* 1992; **23**: 273–9
27 **Epstein JI.** Gleason score 2–4 adenocarcinoma of the prostate on needle biopsy: a diagnosis that should not be made. *Am J Surg Pathol* 2000; **24**: 477–8

Correspondence: Hiroji Uemura, Department of Urology, Yokohama City University Graduate School of Medicine, 3-9 Fukuura, Kanazawa-ku, Yokohama 236-0004, Japan.
e-mail: hu0428@med.yokohama-cu.ac.jp

Abbreviations: **ISUP**, International Society of Urologic Pathology; **RP**, radical prostatectomy; **(C)(I)GS**, (conventional) (ISUP) Gleason score; **NB**, needle biopsy; **BRFS**, biochemical recurrence-free survival.

aPKCλ/ι promotes growth of prostate cancer cells in an autocrine manner through transcriptional activation of interleukin-6

Hitoshi Ishiguro[a,b], Kazunori Akimoto[c], Yoji Nagashima[d,e], Yasuyuki Kojima[f], Takeshi Sasaki[g], Yukari Ishiguro-Imagawa[h], Noboru Nakaigawa[a], Shigeo Ohno[c,e], Yoshinobu Kubota[a,e], and Hiroji Uemura[a,1]

Departments of [a]Urology, [c]Molecular Biology, [d]Molecular Pathology, [f]Gastroenterological Surgery, and [h]Biology and Function in the Head and Neck, Yokohama City University Graduate School of Medicine, 3-9, Fukuura, Kanazawa-ku, Yokohama, Kanagawa 236-0004, Japan; [g]Division of Pathology, Yokohama City University Medical Center, 4-57, Urafune-cho, Minami-ku Yokohama, Kanagawa 232-0024, Japan; [b]Photocatalyst Group, Kanagawa Academy of Science and Technology. 3-2-1, Sakado, Takatsu-ku, Kawasaki, Kanagawa 213-0012, Japan; and [e]Advanced Medical Research Center, Yokohama City University, Yokohama, Kanagawa 236-0004, Japan

Communicated by Tadamitsu Kishimoto, Osaka University, Osaka, Japan, June 25, 2009 (received for review April 8, 2009)

Understanding the mechanism by which hormone refractory prostate cancer (HRPC) develops remains a major issue. Alterations in HRPC include androgen receptor (AR) changes. In addition, the AR is activated by cytokines such as interleukin-6 (IL-6). Atypical protein kinase C (aPKCλ/ι) has been implicated in the progression of several cancers. Herein, we provide evidence that aPKCλ/ι expression correlates with prostate cancer recurrence. Experiments in vitro and in vivo revealed aPKCλ/ι to be involved in prostate cancer cell growth through secretion of IL-6. Further, aPKCλ/ι activates transcription of the IL-6 gene through NFκB and AP-1. We conclude that aPKCλ/ι promotes the growth of hormone independent prostate cancer cells by stimulating IL-6 production in an autocrine manner. Our findings not only explain the link between aPKCλ/ι and IL-6, implicated in the progression a variety of cancers, but also establish a molecular change involved in the development of HRPC. Further, aPKCλ/ι expression might be a biomarker for prostate cancer progression.

IL-6 | PSA | recurrence

Despite earlier detection and recent advances in surgery and radiation, prostate cancer is the second leading cause of cancer deaths in men in western countries (1). Hormone therapy in the form of medical or surgical castration remains the mainstay of systemic prostate cancer treatment. However, despite initial favorable responses to hormone therapy, hormone refractory tumors develop for which there is as yet no effective treatment (2). The androgen receptor (AR) and its signaling remain intact, as demonstrated by the expression of prostate specific antigen (PSA), in androgen-independent cancer cells. Alterations in these cells include AR amplification, AR point mutations, and changes in the expressions of AR co-regulatory proteins (3). In addition, AR can be activated in a ligand-independent fashion by compounds including growth factors and cytokines, such as interleukin-6 (IL-6) (4–6). Understanding the mechanism of androgen-independent prostate cancer development is essential not only for diagnosis but also more effective therapy.

Atypical protein kinase C (aPKCλ/ι and aPKCζ) is a protein kinase C isozyme distinct from other classes of this enzyme, structurally and functionally (7, 8). It plays multifunctional roles in cellular maintenance and growth of epithelial cells, for example, signal transduction and cell polarity (9–15). Studies on lung, ovary, colon, and breast cancers have demonstrated a relationship between aPKCλ/ι expression and cancer progression and suggest that aPKCλ/ι expression might predict poor survival (16–22). There are several reports showing enhanced aPKC expression in human prostate cancer tissues, but the relationship between aPKCλ/ι and prostate cancer progression remains unclear (23, 24). Furthermore, the mechanism by which aPKC promotes the progression of a variety of cancers remains uncertain. Then, we focus on aPKCλ/ι expression and its roles in prostate cancer.

IL-6, a cytokine involved in immune and hematopoietic activities, has been implicated in the progression of a variety of human cancers (25). In prostate cancer, IL-6 has been suggested to play a role in cancer progression, especially that of hormone refractory cancer (26–30). Serum IL-6 is elevated in patients with prostate cancer (28). The IL-6 receptor is expressed in prostate cancer cell lines and IL-6 is secreted only by androgen independent prostate cancer cell lines (27, 29, 30). Although these observations suggest the importance of IL-6 in prostate cancer progression, the mechanism by which IL-6 expression is regulated in prostate cancer cells is not fully understood.

Herein, we investigated aPKCλ/ι expression in 29 clinical prostate cancer tissue specimens and found a correlation between aPKCλ/ι expression and PSA failure, a clinical hallmark of recurrence. Experiments, both in vitro and in vivo, on androgen-independent cancer cells, employing siRNA-mediated depletion of aPKCλ/ι, revealed this isozyme to be involved in the proliferation of prostate cancer cells. The in vitro experiments further showed aPKCλ/ι involvement in the secretion of IL-6 into the culture medium, suggesting cancer cell growth to occur via an autocrine mechanism. This finding demonstrates the link between aPKCλ/ι and IL-6, both of which have been implicated in cancer progression. We also demonstrated that aPKCλ/ι is involved in transcription of the IL-6 gene promoter through activation of NFκB and AP-1, both of which have been implicated in transcription of the IL-6 gene in prostate cancer cells. We conclude that aPKCλ/ι promotes prostate cancer cell growth in an autocrine manner via stimulation of IL-6 production and secretion.

Results

Correlation Between aPKCλ/ι Expression and PSA Failure, a Clinical Marker of Prostate Cancer Recurrence. To clarify the relationship between aPKCλ/ι expression and prostate cancer, we first evaluated aPKCλ/ι expression at the mRNA levels in 29 specimens of human prostate cancer tissues. Clinicopathological features are listed at Table S1. Real-time quantitative PCR (qPCR) analyses revealed that aPKCλ/ι mRNA was more highly expressed in cancer tissue samples than in paired normal controls

Author contributions: H.I., K.A., Y.N., and Y. Kubota designed research; H.I., K.A., Y.N., Y. Kojima, T.S., Y.I.-I., and N.N. performed research; H.I., K.A., Y.N., S.O., Y. Kubota, and H.U. analyzed data; and H.I., K.A., Y.N., S.O., Y. Kubota, and H.U. wrote the paper.

The authors declare no conflict of interest.

[1]To whom correspondence should be addressed: E-mail: hu0428@med.yokohama-cu.ac.jp.

This article contains supporting information online at www.pnas.org/cgi/content/full/0907044106/DCSupplemental.

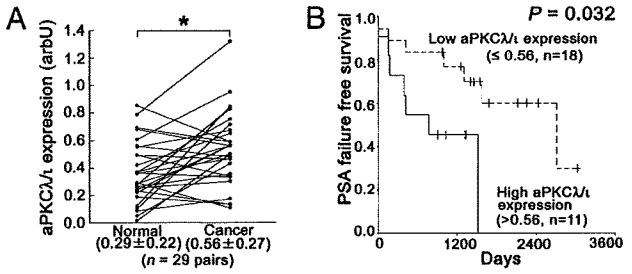

Fig. 1. Relationships between aPKCλ/ι expression in prostate cancer tissues. (*A*) aPKCλ/ι expression was compared between paired prostate cancer and normal (BPH) prostate tissues obtained from same patients (n = 29 pairs). *, P = 0.001 by paired t test. arbU: arbitrary units. Values indicate medians ± SD. (*B*) Kaplan-Meier and log rank analysis of aPKCλ/ι and PSA failure time. aPKCλ/ι expressions in prostate cancer tissues (n = 29) were divided into two groups according to the median value (High: n = 11, >0.56 and Low: n = 18, ≤0.56), and analyzed (P = 0.032 by log rank test).

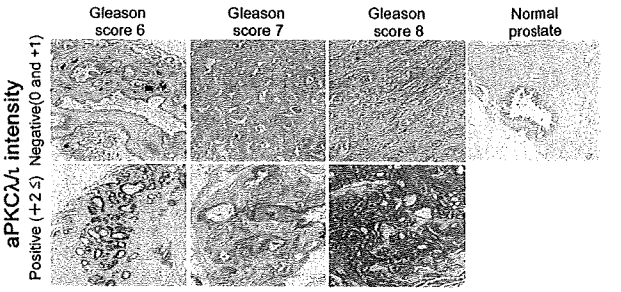

Fig. 2. Representative examples of immunohistochemistry of aPKCλ/ι expression. Expression intensities of aPKCλ/ι were divided in two groups (positive; +2≤ and negative; 0 and + 1). Gleason scores are indicated in the figures and aPKCλ/ι expression in normal prostate tissue is also shown in the figure.

from same patients (Fig. 1*A*, P = 0.001). There were no associations between aPKCλ/ι mRNA expression and certain clinical features (Fig. S1). On the other hand, when the samples were divided into two groups by setting a cut-off at the median aPKCλ/ι value (high: >0.56, n = 11 and low: ≤0.56, n = 18), we recognized a statistically significant correlation between aPKCλ/ι mRNA expression and PSA failure (Fig. 1*B*, P = 0.032). There was no correlation between other clinical features and PSA failure (Fig. S2). Serum PSA was measured every 2–3 months after radical prostatectomy. PSA failure was defined as a continuous elevation with a PSA level greater than 0.2 ng/mL. PSA failure has been suggested to be associated with cancer specific death (31). Thus, aPKC may be a prognostic biomarker for prostate cancer. In univariate and multivariate analyses, only aPKCλ/ι mRNA expression showed statistical significance (Table 1, P = 0.039 in univariate and P = 0.033 in multivariate analysis). Subsequent immunohistochemical analysis of aPKCλ/ι in 43 prostate specimens (cancer tissues; n = 40, and normal tissues; n = 3) confirmed aPKCλ/ι expression at the protein level in normal and tumor tissues, with a variety of intensities (Fig. 2 and Table S2). Immunohistochemical analysis also revealed enhanced staining of aPKCλ/ι to be localized to the cytoplasm in epithelial cells of the prostate, but not in stromal cells, suggesting the importance of the specific expression of aPKCλ/ι protein in epithelial cells of the prostate.

Suppression of aPKCλ/ι Expression Reduces Prostate Cancer Cell Growth In Vitro and In Vivo. The correlation of aPKCλ/ι expression in prostate cancer tissue samples with PSA failure prompted us to clarify the role of aPKCλ/ι in prostate cancer cell lines. Western blot clearly showed aPKCλ/ι expression to be higher in prostate cancer cell lines, LNCaP, PC-3 and DU145 cells, than in normal prostate cells, PrEC, as expected (Fig. 3*A*). To evaluate the role of aPKCλ/ι in cell growth, we introduced siRNA for aPKCλ/ι into the DU145, an androgen-independent cell line, and established a mixture of cell lines expressing siRNA for aPKCλ/ι (DU-P), as well as vector control (DU-C) cells. As shown in Fig. 3*B*, we confirmed the reduced expression of aPKCλ/ι in the pooled transfectant (DU-P), as compared to control cells (DU-C). We found that DU-P cells grew more slowly than control cells (Fig. 3*C*, $P < 0.05$ at days 3 and 4, and $P < 0.01$ at days 5 and 6). We next transplanted the cell lines into nude mice and monitored the tumor volume in vivo. As shown in Fig. 3*D*, the xenografts of aPKCλ/ι-depleted DU-P cells showed slower growth than those of control DU-C cells (P = 0.04 at 5 weeks, P = 0.012 at 6 weeks). The suppression of aPKCλ/ι expression in xenografts was confirmed by RT-PCR analysis (Fig. 3*E*, P = 0.001). Thus, the suppression of aPKCλ/ι expression leads to the inhibition of prostate cancer growth in vitro and in vivo, clearly indicating a positive role of aPKCλ/ι in the growth of prostate cancer cells.

aPKCλ/ι Mediates the Growth of Prostate Cancer Cells in an Autocrine Manner Through IL-6 Secretion. To explore the mechanism involved in aPKCλ/ι-dependent growth of prostate cancer cells, we

Table 1. Relative hazard of recurrence free survival in univariate and multivariate analysis

		Univariate			Multivariate		
		HR	95% CI	P	HR	95% CI	P
aPKCλ/ι expression	≤ 0.56 (n = 18)						
	> 0.56 (n = 11)	3.914	1.071–14.305	0.039	6.768	1.161–39.443	0.033
Stage	pT2 (n = 16)						
	pT3 (n = 13)	2.866	0.747–10.992	0.125	3.928	0.781–19.748	0.097
Histology	Well (n = 5)						
	Moderately (n = 13)	1.129	0.218–5.848	0.885	1.12	0.173–7.275	0.905
	poorly (n = 11)	0.892	0.161–4.932	0.895	0.887	0.081–9.669	0.922
Gleason score	≤ 6 (n = 11)						
	7 (n = 10)	1.087	0.291–4.060	0.901	1.562	0.275–8.876	0.615
	8 and 9 (n = 8)	0.842	0.184–3.866	0.825	4.346	0.346–54.581	0.255
Age	≤ 68 (n = 16)						
	> 68 (n = 13)	1.362	0.393–4.718	0.626	1.946	0.488–7.761	0.346
PSA	≤ 10 (n = 15)						
	> 10 (n = 14)	1.168	0.375–3.639	0.789	0.931	0.233–3.721	0.920

CI, confidence interval; HR, hazard ratio.

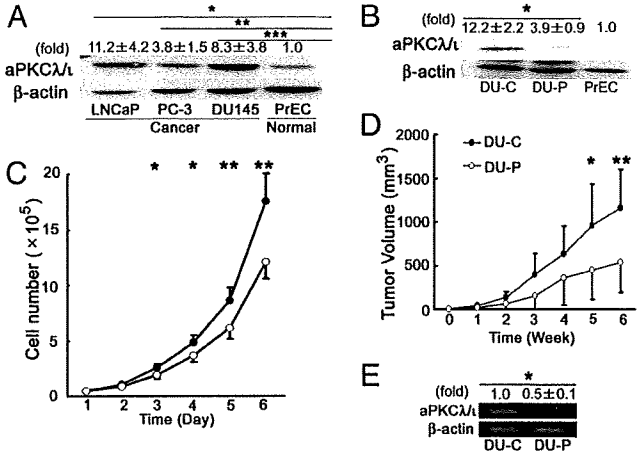

Fig. 3. aPKCλ/ι expression in prostate cancer cell lines and growth inhibition of aPKCλ/ι siRNA transfected DU145 cells in vitro and in vivo. (*A*) aPKCλ/ι expression in prostate cell lines was analyzed by Western blot. β-actin was used as an internal control. Values indicate means ± SD at least three independent experiments (set as 1.0 in PrEC). *, $P = 0.017$, **, $P = 0.032$ and ***, $P = 0.031$ by unpaired *t* test. (*B*) DU145 cells transfected with siRNA for aPKCλ/ι expression vector (DU-P cells) and empty vector (DU-C cells) were confirmed by Western blot. β-actin was used as an internal control. Values indicate means ± SD from at least three independent experiments (set as 1.0 in PrEC). *, $P = 0.004$ by unpaired *t* test. (*C*) The inhibition of cell growth of siRNA transfected cells in vitro. DU-C (filled circles) and DU-P (open circles) cells were seeded onto 12-well plates at 4×10^4 cells and counted until day 6 ($n = 4$ in each group). Points and bars indicate means ± SD from at least three independent experiments. *, $P < 0.05$ **, $P < 0.01$ by unpaired *t* test. (*D*) The inhibition of cell growth of siRNA transfected cells in vivo. DU-C (filled circles) and DU-P (open circles) cells were implanted s.c. into the right and left flanks of male nude mice ($n = 7$ in each group) and tumor growth was calculated at 6 weeks (The day of injection was taken as week 0). Points and bars indicate means ± SD. *, $P = 0.04$; **, $P = 0.012$ by unpaired *t* test. (*E*) aPKCλ/ι mRNA expression extracted from xenografts. Total RNA was extracted from the same tumor specimens and aPKCλ/ι mRNA expression was examined. Values indicate means ± SD from at least three independent experiments (set as 1.0 in DU-C derived tumors) *, $P = 0.001$ by unpaired *t* test.

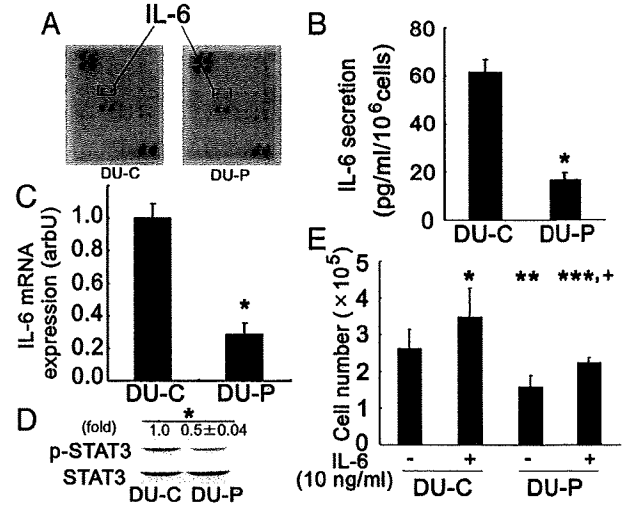

Fig. 4. IL-6 expression was suppressed in siRNA transfected prostate cancer cells. (*A*) Conditioned media from DU-C and DU-P cells were analyzed using a membrane array. Arrows show IL-6 spots. Since this representative data are screening test only, it is performed once. This data had confirmed using ELISA and qPCR. (*B*) Expressions of IL-6 protein in DU-C and DU-P cells were confirmed using ELISA. Conditioned media from DU-C and DU-P ($n = 2$ in each group) were analyzed using an IL-6 ELISA kit from R&D Systems. Bars represent means ± SD from at least three independent experiments. *, $P = 0.002$ by unpaired *t* test. (*C*) Expressions of IL-6 mRNA in DU-C and DU-P cells. IL-6 mRNA expression was investigated by qPCR ($n = 3$ in each group). Bars represent means ± SD from at least three independent experiments. *, $P < 0.001$ by unpaired *t* test. arbU: arbitrary units. (*D*) STAT3 phosphorylations in DU-C and DU-P cells were analyzed by Western blot. After phospho-STAT3 protein had been detected, membranes were re-probed for STAT-3, and then used as controls. Values indicate means ± SD at least three independent experiments (set as 1.0 in DU-C). *, $P = 0.002$ by unpaired *t* test. (*E*) Recombinant IL-6 stimulated growth of DU-C and DU-P cells. DU-C and DU-P cells were stimulated with IL-6 (10 ng/ml). At day 3 after stimulation, cells were treated with trypsin and counted ($n = 4$ in each group). Bars represent means ± SD from at least three independent experiments. *, $P = 0.001$, **, $P < 0.001$ and ***, $P = 0.393$ (vs. DU-C without IL-6 stimulation) $^+$, $P = 0.016$ (vs. DU-P without IL-6 stimulation) by ANOVA followed by Bonferroni test.

focused on cytokines which have been implicated in the growth of a variety of cancer cells. Comparison of the conditioned medium between DU-C and DU-P cell lines by cytokine membrane array revealed IL-6 to be a candidate cytokine, that is, that its regulation might be under the control of aPKCλ/ι (Fig. 4*A*). The ELISA results confirmed that IL-6 is secreted into conditioned medium of control DU-C cells and decreased in aPKCλ/ι-depleted DU-P cells (Fig. 4*B*, $P = 0.002$). Similarly, qPCR revealed IL-6 mRNA expression to also be suppressed in aPKC-depleted DU-P cells (Fig. 4*C*, $P < 0.001$). These results show that aPKCλ/ι regulates IL-6 secretion in prostate cancer cells.

IL-6 is the cytokine reportedly expressed in androgen-independent prostate cancer cell lines including parental DU145 (26, 30). We next examined the effect of aPKCλ/ι depletion on phosphorylation of STAT3, one of the downstream mediators of the possible IL-6 involvement in prostate cancer cells (25, 29, 32, 33). As shown in Fig. 4*D*, STAT3 phosphorylation was down-regulated in DU-P cells as compared to DU-C cells, indicating that IL-6 signaling is altered in aPKCλ/ι-depleted cells. Given that aPKCλ/ι depletion results in the decreased production of IL-6, these results raise another question as to whether aPKCλ/ι depletion also affects IL-6 signaling, versus only IL-6 production. To clarify this issue, we next evaluated the response of cells to ectopic IL-6. When both cell types were treated with recombinant IL-6 (10 ng/ml) for 3 days, IL-6 increased cell growth, as we expected (Fig. 4*E*, $P = 0.001$ and $P = 0.016$). Moreover, DU-P cells treated with IL-6 showed growth similar to that of DU-C cells not treated with IL-6 (Fig. 4*E*, $P = 0.393$). Thus, aPKCλ/ι depletion does not affect the growth response of cells to IL-6. Taking these observations together, we conclude that secretion of IL-6 enhanced by aPKCλ/ι expression plays a role in promoting growth of the prostate cancer cell line DU145. Our results suggest that this growth promotion is mediated in an autocrine manner.

aPKCλ/ι Mediates IL-6 Gene Transcription Through NFκB and AP-1 in Prostate Cancer Cells. To analyze the mechanism by which aPKCλ/ι enhances IL-6 secretion, we next examined the effect of aPKCλ/ι on transcription of the IL-6 gene by luciferase reporter assay and EMSA. The luciferase reporter gene, pGL4-IL6p, contains a 1.2-kb 5′-flanking region of genomic DNA isolated from DU145 cells. This region contains the regulatory sequences recognized by AP-1, NFκB, MRE and other factors (30). As shown in Fig. 5*A*, overexpression of aPKCλ/ι in DU145 cells enhanced activation of the IL-6 promoter (Fig. 5*A*, $P = 0.016$). On the other hand, depletion of aPKCλ/ι (DU-P cells) resulted in decreased reporter gene expression (Fig. 5*B*, $P < 0.001$). These results strongly support the notion that aPKCλ/ι is involved in transcription of the IL-6 gene. Transcription of this gene is regulated by two major transcription factors, AP-1 and NFκB, in prostate cancer cells (30). To examine the involvement of these transcription factors in aPKCλ/ι-mediated IL-6 gene

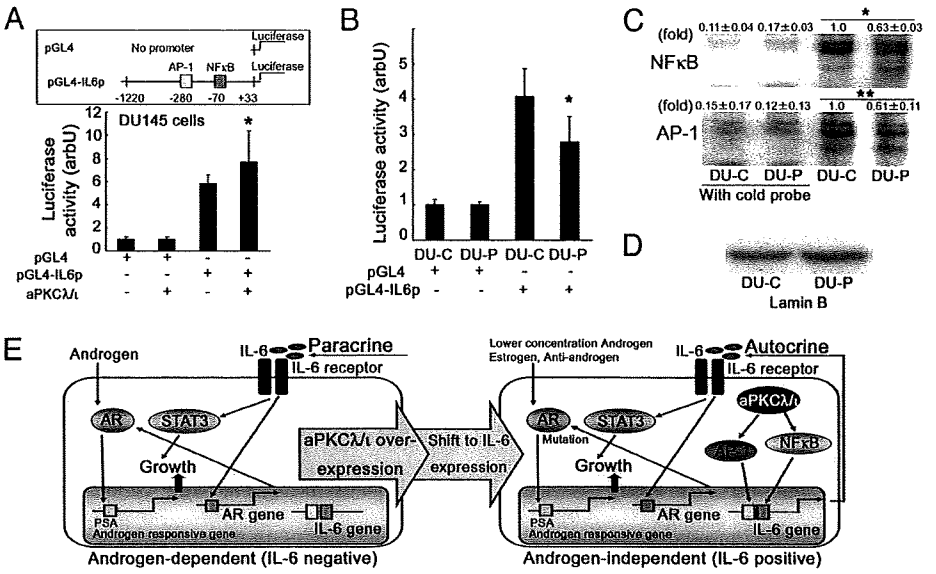

Fig. 5. Involvement of aPKCλ/ι in activation of the IL-6 gene promoter and its transcription factors, NFκB and AP-1. (*A*) IL-6 promoter activation was induced by wild type aPKCλ/ι in DU145 cells. DU145 cells were transfected with pGL4, pGL4-IL6p, empty vector and wild type aPKCλ/ι. After a 48 h incubation, luciferase activity was analyzed in a luminometer ($n = 4$ in each group). Each control was given a value of 1.0 and each bar indicates the means ± SD of at least three independent experiments. *, $P = 0.016$ (vs. pGL4-IL6p without wild-type aPKCλ/ι expression vector) by ANOVA following Bonferroni test. (*B*) IL-6 promoter activation was reduced in DU-P cells. DU-C and DU-P cells were transfected with pGL4 and pGL4-IL6p. After a 12-h incubation, luciferase activity was analyzed in a luminometer ($n = 4$ in each group). Each control was given a value of 1.0 and each bar indicates the means ± SD of at least three independent experiments. *, $P < 0.001$ (vs. DU-C with pGL4-IL6p transfection) by ANOVA following Bonferroni test. (*C*) DNA binding properties of NFκB and AP-1 were examined by EMSA. Each nuclear extract was reacted with ^{32}P-labeled specific probes. To confirm specific binding of nuclear extracts and probes, reactions were also carried out using a cold probe. Values indicate means ± SD at least three independent experiments (set as 1.0 in DU-C). *, $P < 0.001$ and **, $P = 0.026$ by ANOVA following Bonferroni test. (*D*) Nuclear extracts for EMSA were confirmed by lamin B immunoblot. (*E*) Autocrine mechanism of prostate cancer cell growth involving aPKCλ/ι and IL-6. Overexpression of aPKCλ/ι in prostate cancer cells leads to up-regulation of IL-6 transcription through NFκB and AP-1 activation. Secreted IL-6 stimulates cell growth through STAT3 activation in an autocrine manner.

transcription, we used EMSA. The results showed both NFκB and AP-1 to be reduced upon aPKCλ/ι depletion (Fig. 5 *C* and *D*, $P < 0.001$ and $P = 0.026$). These results support the notion that both AP-1 and NFκB are involved in aPKCλ/ι-mediated transcriptional activation of the IL-6 gene.

Discussion

aPKCλ/ι overexpression has been implicated in the progression and invasiveness of several tumor types including non-small cell lung cancer, ovarian cancer, breast cancer and glioma (16–22, 34, 35). Gene amplification of aPKCλ/ι is also observed in some cases (16, 18). In this study, we obtained evidence supporting a statistically significant correlation between aPKCλ/ι overexpression and a clinical marker of prostate cancer recurrence, PSA failure. A very recent study demonstrated aPKCλ/ι expression is required for cell survival (36). Thus, the aPKCλ/ι expression level and its activity might be prognostic factors for PSA failure.

IL-6, as noted above, has been implicated in the progression of a variety of tumors including prostate cancer (25–27, 29). Its overexpression has been detected in tissues (37, 38) and serum (28) from cancer patients. Preoperative plasma IL-6 level is related to PSA failure after radical prostatectomy (39). In vivo study indicates an important role of IL-6 in prostate cancer cells. Inhibition of IL-6 by anti-IL-6 antibody decreases the growth of PC-3 cells, which is one of an androgen-independent prostate cancer cells, in vivo (40). Therefore, IL-6 may play a role in androgen-independent growth of prostate cancer. Our findings on the molecular link between aPKCλ/ι and IL-6 raise an intriguing question as to the correlation between aPKCλ/ι expression and IL-6 expression in prostate cancer patients. We evaluated our tissue samples for IL-6 expression by qPCR. However, there was no statistically significant correlation between aPKCλ/ι expression and IL-6 expression (Fig. S3). One explanation is that the examined tissues contained not only cancer cells but also stromal cells. In support of this possibility, most prostate cancer tissues that express high levels of aPKCλ/ι protein (30/43, 70%) show a specific overexpression in epithelial cells but not in the surrounding stromal cells. However, IL-6 is reportedly expressed not only in prostate cancer epithelial cells, but also in stromal cells (37, 38). Thus, the use of laser capture microdissection (LCM) might be required to clarify this point. Unfortunately, we did not have sufficient sample quantities for LCM. We are currently conducting more extensive clinical studies aimed at clarifying the correlation between aPKCλ/ι expression and IL-6 expression.

Experiments using the prostate cancer cell line DU145 revealed that aPKCλ/ι is involved in prostate cancer growth both in vivo and in vitro. Furthermore, depletion of aPKCλ/ι in DU145 cells suppressed NFκB and AP-1 activities, transcription and secretion of IL-6, as well as suppressing cell growth, but not IL-6 signaling. We conclude that enhanced aPKCλ/ι expression in prostate cancer cells results in overproduction and secretion of a prostate growth factor, IL-6, at the transcriptional level. This forms an autocrine loop contributing to the growth of prostate cancer (Fig. 5*E*). The aPKC-dependent expression of IL-6 mRNA is also observed for another androgen-independent prostate cell line, PC-3, suggesting the generality of this regulation (Fig. S4). The specific overexpression of aPKCλ/ι in epithelial cells but not in stromal cells of the prostate further supports such an autocrine mechanism. It is known that most of androgen-independent prostate cancer tissues overexpress or/and express mutated AR that is still activated by lower concentration androgen, estrogen and anti-androgen drug (3). Taken together, the pathway might cooperate with the deregulated AR

system to regulate proliferation of hormone-independent prostate cancer cells (Fig. 5*E*).

The following reports strongly support our conclusion. Combined constitutive activation of NFκB and AP-1 has been reported to mediate deregulated expression of IL-6 in DU145 cells (30). Ectopic expression of IL-6 in IL-6-negative LNCaP prostate cancer cells results in stimulation of the STAT3 signaling pathway as well as cell growth (29). However, the mechanism by which IL-6 expression is deregulated is not yet fully understood. As for aPKCλ/ι, several studies have shown that aPKCλ/ι activates NFκB and AP-1 (9, 10, 13–15, 41–44). Furthermore, aPKC activates NFκB in prostate cells (45). aPKC deregulates the growth of mouse prostate cancer cells (46). While the mechanism by which aPKC affects the growth of cancer cells remains obscure, the involvement of Rho B suppression in aPKC-dependent invasive properties in glioblastoma (35) and that of activation of the Rac1/Erk pathway in aPKC-dependent growth and tumorigenicity have been reported (17, 22). Our present results may explain the link between aPKCλ/ι and IL-6, two molecules implicated in the progression of a variety of malignancies, and establish a molecular mechanism underlying prostate cancer development and/or progression, thereby providing insights into the prognosis and treatment of prostate cancer.

How aPKCλ/ι expression was regulated in prostate cancer cells? Amplification of aPKCλ/ι gene is reported in lung and ovarian cancer (16, 18, 19) and amplification of chromosome 3q including aPKCλ/ι gene in prostate cancer cell lines (47). Another possibility is that aPKCλ/ι expression is up-regulated through the transcriptional activation of aPKCλ/ι promoter during hormone refractory process. Gustafson et al. reported aPKCλ/ι promoter analysis using luciferase (48). They show Bcr-Abl regulates aPKCλ/ι expression through the MEK-dependent activation of an Elk1 element within aPKCλ/ι promoter in leukemia cell line. We are ongoing the investigation of the mechanism of aPKCλ/ι overexpression involving in hormone refractory process. Further, other molecules expression, such as PAR-4, might be affected the alteration of aPKCλ/ι activity during hormone refractory process (49).

One of the most important clinical aspects of prostate cancer is dramatically decreased androgen-dependent cell growth, a typical indicator of prostate cancer progression. Possible mechanisms include androgen receptor overexpression and other mutations that result in hypersensitivity to androgens and/or other growth factors (3–6). IL-6 is overexpressed in hormone refractory prostate cancer patients and is one of the factors implicated in this process (26–28, 37). Importantly, IL-6 can stimulate androgen receptor activation independently of androgens with the induction of androgen receptor expression (4, 5). A recent study on LNCaP cells, which are sensitive to androgens and do not usually express IL-6, suggested IL-6 to be involved in the progression of prostate cancer cells from androgen dependence to androgen independence (50). It has been reported androgen-dependent prostate cancer cells obtained from xenografts treated with the anti-IL-6 antibody retained in androgen-dependence. In contrast, cancer cells obtained from xenografts untreated with the anti-IL-6 antibody are converted to androgen-independence in vitro and in vivo experiments, which means that IL-6 contributes to the development of androgen independence in prostate cancer (51). Taking these observations and our results together, we speculate that the molecular link between aPKCλ/ι and IL-6 revealed in the present study supports the notion that aPKCλ/ι is involved in this transition from androgen dependent to androgen independent growth of prostate cancer. As for the relationship between androgens and aPKC, there is an interesting report suggesting that aPKCζ, another aPKC isotype, is involved in the growth of androgen dependent LNCaP cells (52). In LNCaP cells, androgen stimulates aPKCζ through an unknown mechanism, and AILNCaP, a LNCaP subline established after androgen depletion, showed constitutive activation of aPKCζ. Another study on a breast cancer cell line, MCF7, showed the involvement of aPKCζ in estradiol-dependent cell growth (53). These reports further suggest a close relationship between aPKC and hormone-dependent cell growth. Our present findings provide additional evidence clarifying this point and are anticipated to facilitate understanding the progression of hormone-related malignancies including prostate cancer. Furthermore, aPKCλ/ι expression might be a biomarker for prostate cancer progression.

Materials and Methods

Cell Lines, Patients, and Tissues Sample. LNCaP, PC-3, and DU145 cells were obtained from the American Type Culture Collection. PrEC cells were obtained from Clonetics. All cell lines were maintained with suitable medium (F-12 supplemented with 10% FCS (FCS) for LNCaP and PC-3, MEM supplemented with 10% FCS for DU145, PrEGM for PrEC) under 5% CO_2.

Paired human untreated primary prostate cancer tissues and normal (or benign prostatic hypertrophy (BPH)) ($n = 29$) tissues from same patients were obtained during radical prostatectomy at Yokohama City University Hospital and its affiliates. The sampling and usage of all prostate tissues in this study were approved by the ethical committee of Yokohama City University Graduate School of Medicine and performed only after obtaining informed consent from each patient. For details, see *SI Text* and Table S1.

Reagents. Human recombinant IL-6 was purchased from R&D Systems. G418 was purchased from Invitrogen Corp. Anti-aPKCι antibody was purchased from BD Biosciences. Anti-lamin-B antibody (c-19) was purchased from Santa Cruz Biotechnology Inc. Anti-actin antibody (AC-15) was purchased from Sigma-Aldrich. Anti-phospho-STAT3 and anti-STAT3 (#9131 and #9132, respectively) antibodies were purchased from Cell Signaling Technology Inc. Anti-rabbit and anti-mouse horseradish peroxidase conjugates were purchased from GE Healthcare U.K. Ltd.

Generation of Stable Transfectant-Induced siRNA for aPKCλ/ι. To investigate the role of aPKCλ/ι in prostate cancer, we generated aPKCλ/ι knock-down cells using siRNA for aPKCλ/ι. The pEB6-Super vector (54) encoding the shRNA sequence for aPKCλ/ι RNAi with the target sequence 5′-CAA GTG TTC TGA AGA GTT T-3′ (DU-P cells) or empty vector (DU-C cells) was transfected into DU145 cells using Nucleofactor electroporation methods (Amaxa AG). Then, transfected cells were selected by G418 (800 μg/mL) over a 3-week period. After the specific down-regulation of aPKCλ/ι had been confirmed by Western blot, the cells were used for further experiments.

RNA Extraction and Real-Time Quantitative PCR (qPCR). Total RNA from cell lines, prostate tissues and xenografts were extracted using ISOGEN (Nippon-Gene) according to the manufacturer's instructions. After cDNA had been synthesized with random hexomers and MMLV (Moloney Murine Leukemia Virus), qPCR was performed with an iCycler and SYBR Green Supermix (Bio-Rad). For details, see *SI Text*.

Immunohistochemistry. Immunohistochemistry was performed for aPKCλ/ι protein expression according to the previous report (20). For details, see *SI Text*.

Cell Growth Analysis. DU-C or DU-P cells (4×10^4) were incubated in 12-well plates (day 0). Incubated cells were harvested with trypsin and counted till 6 days (from day 1 to day 6) using a hematocytometer (Beckman Coulter, Inc.). For the IL-6 stimulation experiment, 4×10^4 DU-C or DU-P cells were seeded onto 12-well plates and incubated for 24 h. The medium was then changed to phenol red-free RPMI1640 with 0.1% BSA (BSA), IL-6 (10 ng/mL) was added and incubation was continued for another 3 days. Then, cells were harvested with trypsin and counted.

In Vivo Tumor Growth. 5×10^6 cells (DU-C and DU-P cells) were injected into the flank regions of athymic nude mice (4–6 weeks old, $n = 7$). Tumors were measured weekly with a caliper (for comparison with the week 0 value). The tumor volume was calculated using the formula: tumor volume (mm^3) = 0.5 × length × (width)^2. After 6 weeks, tumors were isolated and aPKCλ/ι expression was confirmed by RT-PCR.

Cytokine Membrane Array. Cytokines in the conditioned medium were detected using Human Cytokine Array III (Ray Biotech) according to the manufacturer's instructions. For details, see *SI Text*.

ELISA (ELISA) for IL-6 Secretion. IL-6 secretion in the collected medium was measured using a human IL-6 ELISA kit according to the manufacturer's instructions (R&D Systems). For details, see *SI Text*.

Western Blot. Cell lysates were prepared and subjected to Western blot. For details, see *SI Text*.

Luciferase Assay. Approximately 1.2 kb of the IL-6 5′-flanking region was generated using PCR from genomic DNA extracted from DU145 cells, and cloned into the pGL4.0 [*luc2*] vector (pGL4-IL6p) (Promega). Wild type aPKCλ/ι was obtained as described in previous reports (9, 10). phRL-SV40 was used as the internal control for the luciferase assay (Promega). After cells transfected each plasmid vector were incubated and lysed, luciferase activity was measured using the dual-luciferase reporter assay system (Promega) and a luminometer, TD-20/20 (Turner Design). For details, see *SI Text*.

Electrophoretic Mobility Shift Assay (EMSA). Nuclear proteins of DU-C or DU-P were extracted using NE-PER (Pierce Biotechnology Inc.) and subjected to EMSA using gel shift assay systems (Promega). For details, see *SI Text*.

Statistical Analysis. All statistical analyses were performed using SPSS for windows (SPSS Inc.). For details, see *SI Text*.

ACKNOWLEDGMENTS. We thank R. Shimizu, Y. Nakamura, T. Yamaki, Y. Imano, T. Taniguchi, H. Soeda, C. Kondo, and A. Ishiyama for technical and secretarial assistance. This work was supported by Grants-in-Aid for Scientific Research from the Ministry of Education, Culture, Science, and Technology; a COE Research Grant from the Japan Society for the Promotion of Science; and a Grant for Strategic Research Promotion from Yokohama City University.

1. Jemal A, et al. (2007) Cancer statistics, 2007. *CA Cancer J Clin* 57:43–66.
2. Calabrò F, Sternberg CN (2007) Current indications for chemotherapy in prostate cancer patients. *Eur Urol* 51:17–26.
3. Taplin ME, Balk SP (2004) Androgen receptor: A key molecule in the progression of prostate cancer to hormone independence. *J Cell Biochem* 91:483–490.
4. Culig Z, Bartsch G, Hobisch A (2002) Interleukin-6 regulates androgen receptor activity and prostate cancer cell growth. *Mol Cell Endocrinol* 197:231–238.
5. Lin DL, Whitney MC, Yao Z, Keller ET (2001) Interleukin-6 induces androgen responsiveness in prostate cancer cells through up-regulation of androgen receptor expression. *Clin* Cancer Res 7:1773–1781.
6. Zhu ML, Kyprianou N (2008) Androgen receptor and growth factor signaling cross-talk in prostate cancer cells. *Endocr Relat Cancer* 15:841–849.
7. Akimoto K, et al. (1994) A new member of the third class in the protein kinase C family, PKC lambda, expressed dominantly in an undifferentiated mouse embryonal carcinoma cell line and also in many tissues and cells. *J Biol Chem* 269:12677–12683.
8. Nishizuka Y (1995) Protein kinase C and lipid signaling for sustained cellular responses. *FASEB J* 9:484–496.
9. Akimoto K, et al. (1996) EGF or PDGF receptors activate atypical PKCλ through phosphatidylinositol 3-kinase. *EMBO J* 15:788–798.
10. Akimoto K, et al. (1998) Atypical protein kinase Cλ binds and regulates p70 S6 kinase. *Biochem J* 335:417–424.
11. Suzuki A, Akimoto K, Ohno S (2003) Protein kinase C λ/ι (PKCλ/ι): aPKC isotype essential for the development of multicellular organism. *J Biochem* 133:9–16.
12. Ohno S (2001) Intercellular junctions and cellular polarity: The PAR-aPKC complex, a conserved core cassette playing fundamental roles in cell polarity. *Curr Opin Cell Biol* 13:641–648.
13. Diaz-Meco MT, et al. (1993) A dominant negative protein kinase C zeta subspecies blocks NF-kappa B activation. *Mol Cell Biol* 13:4770–4775.
14. Moscat J, Diaz-Meco MT, Albert A, Campuzano S (2006) Cell signaling and function organized by PB1 domain interactions. *Mol Cell* 23:631–640.
15. Sanz L, Sanchez P, Lallena MJ, Diaz-Meco MT, Moscat J (1999) The interaction of p62 with RIP links the atypical PKCs to NFκB activation. *EMBO J* 18:3044–3053.
16. Regala RP, et al. (2005) Atypical protein kinase C ι is an oncogene in human non-small cell lung cancer. *Cancer Res* 65:8905–8911.
17. Regala RP, et al. (2005) Atypical protein kinase C ι plays a critical role in human lung cancer cell growth and tumorigenicity. *J Biol Chem* 280:31109–31115.
18. Eder AM, et al. (2005) Atypical PKC iota contributes to poor prognosis through loss of apical-basal polarity and cyclin E overexpression in ovarian cancer. *Proc Natl Acad Sci USA* 102:12519–12524.
19. Zhang L, et al. (2006) Integrative genomic analysis of protein kinase C (PKC) family identifies PKCiota as a biomarker and potential oncogene in ovarian carcinoma. *Cancer Res* 66:4627–4635.
20. Kojima Y, et al. (2008) The overexpression and altered localization of the atypical Protein kinase C lambda/iota in breast cancer correlates with the pathological type of these tumors. *Human Pathol* 39:824–831.
21. Li Q, et al. (2008) Correlation of aPKC-iota and E-cadherin expression with invasion and prognosis of cholangiocarcinoma. *Hepatobiliary Pancreat Dis Int* 7:70–75.
22. Murray NR, et al. (2004) Protein kinase C is required for Ras transformation and colon carcinogenesis in vivo. *J cell Biol* 164:797–802.
23. Cornford P, et al. (1999) Protein kinase C isoenzyme patterns characteristically modulated in early prostate cancer. *Am J Pathol* 154:137–144.
24. Koren R, et al. (2004) Expression of protein kinase C isoenzymes in benign hyperplasia and carcinoma of prostate. *Oncol Rep* 11:321–326.
25. Hong DS, Angelo LS, Kurzrock R (2007) Interleukin-6 and its receptor in cancer: implications for translational therapeutics. *Cancer* 110:1911–1928.
26. Okamoto M, Lee C, Oyasu R (1997) Interleukin-6 as a paracrine and autocrine growth factor in human prostatic carcinoma cells in vitro. *Cancer Res* 57:141–146.
27. Corcoran NM, Costello AJ (2003) Interleukin-6: Minor player or starring role in the development of hormone-refractory prostate cancer ? *BJU Int* 91:545–553.
28. Nakashima J, et al. (2000) Serum interleukin 6 as a prognostic factor in patients with prostate cancer. *Clin* Cancer Res 6:2702–2706.
29. Lou W, Ni Z, Dyer K, Tweardy DJ, Gao AC (2000) Interleukin-6 induces prostate cancer cell growth accompanied by activation of stat3 signaling pathway. *Prostate* 42:239–242.
30. Zerbini LF, Wang Y, Cho JY, Libermann TA (2003) Constitutive activation of nuclear factor κB p50/p65 and Fra-1 and JunD is essential for deregulated interleukin 6 expression in prostate cancer. *Cancer Res* 63:2206–2215.
31. Freedland SJ, et al. (2005) Risk of prostate cancer-specific mortality following biochemical recurrence after radical prostatectomy. *JAMA* 294:433–439.
32. Heinrich PC, et al. (2003) Principles of interleukin (IL)-6-type cytokine signaling and its regulation. *Biochem J* 374:1–20.
33. Tam L, et al. (2007) Expression levels of the JAK/STAT pathway in the transition from hormone-sensitive to hormone-refractory prostate cancer. *Br J Cancer* 97:378–383.
34. Patel R, et al. (2008) Involvement of PKC-iota in glioma proliferation. *Cell Prolif* 41:122–135.
35. Baldwin RM, Parolin DA, Lorimer IA (2008) Regulation of glioblastoma cell invasion by PKC iota and RhoB. *Oncogene* 27:3587–3595.
36. Win HY, Acevedo-Duncan M (2009) Role of protein kinase C-iota in transformed non-malignant RWPE-1 cells and androgen-independent prostate carcinoma DU-145 cells. *Cell Prolif* 42:182–194.
37. Hobisch A, et al. (2000) Immunohistochemical localization of interleukin-6 and its receptor in benign, premalignant and malignant prostate tissue. *J Pathol* 191:239–244.
38. Royuela M, et al. (2004) Immunohistochemical analysis of the IL-6 family of cytokines and their receptors in benign, hyperplasic, and malignant human prostate. *J Pathol* 202:41–49.
39. Shariat SF, et al. (2001) Plasma levels of interleukin-6 and its soluble receptor are associated with prostate cancer progression and metastasis. *Urology* 58:1008–1015.
40. Smith PC, Keller ET (2001) Anti-interleukin-6 monoclonal antibody induces regression of human prostate cancer xenografts in nude mice. *Prostate* 48:47–53.
41. Huang C, et al. (2001) Inhibition of atypical PKC blocks ultraviolet-induced AP-1 activation by specifically inhibiting ERKs activation. *Mol Carcinog* 27:65–75.
42. Lu Y, Jamieson L, Brasier AR, Fields AP (2001) NF-kappaB/RelA transactivation is required for atypical protein kinase C iota-mediated cell survival. *Oncogene* 20:4777–4792.
43. Bonizzi G, Piette J, Schoonbroodt S, Merville MP, Bours V (1999) Role of the protein kinase C λ/ι isoform in nuclear factor-κB activation by interleukin-1β or tumor necrosis factor-α: cell type specificities. *Biochem Pharmacol* 57:713–720.
44. Lallena MJ, Diaz-Meco MT, Bren G, Payá CV, Moscat J (1999) Activation of IκB kinase β by protein kinase C isoforms. *Mol Cell Biol* 19:2180–2188.
45. Win HY, Acevedo-Duncan M (2008) Atypical protein kinase C phosphorylates IKKαβ in transformed non-malignant prostate cell survival. *Cancer Lett* 270:302–311.
46. Ghosh PM, Bedolla R, Mikhailova M, Kreisberg JI (2002) RhoA-dependent murine prostate cancer cell proliferation and apoptosis: Role of protein kinase Czeta. *Cancer Res* 62:2630–2636.
47. Nupponen NN, Hyytinen ER, Kallioniemi AH, Visakorpi T (1998) Genetic alterations in prostate cancer cell lines detected by comparative genomic hybridization. *Cancer Genet Cytogenet* 101:53–57.
48. Gustafson WC, et al. (2004) Bcr-Abl regulates protein kinase Cι (PKCι) transcription via an Elk1 site in the PKCι promoter. *J Biol Chem* 279:9400–9408.
49. Gurumurthy S, Rangnekar VM (2004) Par-4 inducible apoptosis in prostate cancer. *J Cell Biol* 91:504–512.
50. Lee SO, Chun JY, Nadiminty N, Lou W, Gao AC (2007) Interleukin-6 undergoes transition from growth inhibitor associated with neuroendocrine differentiation to stimulator accompanied by androgen receptor activation during LNCaP prostate cancer cell progression. *Prostate* 67:764–773.
51. Wallner L, et al. (2006) Inhibition of interleukin-6 with CNTO328, an anti-inteleukin-6 monoclonal antibody, inhibits conversion of androgen-dependent prostate cancer to an androgen-independent phonotype in orchiectomized mice. *Cancer Res* 66:3087–3095.
52. Inoue T, et al. (2006) Requirement of androgen-dependent activation of protein kinase Cζ for androgen-dependent cell proliferation in LNCaP cells and its roles in transition to androgen-independent cells. *Mol Endocrinol* 20:3053–3069.
53. Castoria G, et al. (2004) Role of atypical protein kinase C in estradiol-triggered G1/S progression of MCF-7 cells. *Mol Cell Biol* 24:7643–7653.
54. Suzuki A, et al. (2004) aPKC acts upstream of PAR-1b in both the establishment and maintenance of mammalian epithelial polarity. *Curr Biol* 14:1425–1435.

Avid F-18 FDG Uptake in Prostatic Sarcoma

Ryogo Minamimoto, MD, PhD, Ukihide Tateishi, MD, PhD,* Hiroji Uemira, MD, PhD,† Shoji Yamanaka, MD, PhD,‡ Yoshinobu Kubota, MD, PhD,† and Tomio Inoue, MD**

Abstract: We report the F-18 FDG PET appearance of an adult prostatic sarcoma. A 76-year-old man with a history of prostate cancer treated by hormone therapy, a lobulated heterogeneous mass in the prostate gland was found on a follow-up pelvic computed tomography. Although the prostate-specific antigen level was within the normal range, transperineal core needle biopsy was performed because recurrent prostatic carcinoma was suspected. The tumor was pathologically diagnosed as a prostatic sarcoma with no evidence of existing prostatic carcinoma. F-18 FDG-PET revealed avid-FDG uptake (maximum SUV of 7.1) and no evidence of distant metastasis.

Key Words: prostatic sarcoma, [F-18]fluorodeoxyglucose, positron emission tomography

(*Clin Nucl Med* 2009;34: 388–389)

Received for publication December 25, 2008; accepted February 8, 2009.

From the Departments of *Radiology, and †Urology, Graduate School of Medicine, Yokohama City University, Yokohama, Japan; and ‡Division of Anatomic and Surgical Pathology, Hospital of Yokohama City University, Yokohama City University School of Medicine, Yokohama, Japan.

Reprints: Ryogo Minamimoto, MD, PhD, Department of Radiology, Yokohama City University, Graduate School of Medicine, 3-9 Fukuura, Kanazawa-ku, Yokohama-shi, Kanagawa-ken, Japan 236-0004. E-mail: ryogom@yokohama-cu.ac.jp.

ISSN: 0363-9762/09/3406-0388

REFERENCES

1. D'Amico AV, Chen MH, Cox MC, et al. Prostate-specific antigen response duration and risk of death for patients with hormone-refractory metastatic prostate cancer. *Urology*. 2005;66:571–576.
2. Schröder FH, van der Cruijsen-Koeter I, de Koning HJ, et al. Prostate cancer detection at low prostate specific antigen. *J Urol*. 2000;163:806–812.
3. Young MD, Dahm P, Robertson CN. Prostatic sarcoma with rapid tumor progression after nerve sparing radical cystoprostatectomy. *J Urol*. 2001;166: 994.
4. Schwarzbach MH, Dimitrakopoulou-Strauss A, Willeke F, et al. Clinical value of [18-F] fluorodeoxyglucose positron emission tomography imaging in soft tissue sarcomas. *Ann Surg*. 2000;231:380–386.
5. Umesaki N, Tanaka T, Miyama M, et al. Positron emission tomography with (18)F-fluorodeoxyglucose of uterine sarcoma: a comparison with magnetic resonance imaging and power Doppler imaging. *Gynecol Oncol*. 2001;80: 372–377.
6. Sung J, Espiritu JI, Segall GM, et al. Fluorodeoxyglucose positron emission tomography studies in the diagnosis and staging of clinically advanced prostate cancer. *BJU Int*. 2003;92:24–27.
7. Hricak H, Choyke PL, Eberhardt SC, et al. Imaging prostate cancer: a multidisciplinary perspective. *Radiology*. 2007;243:28–53.
8. Kao PF, Chou YH, Lai CW. Diffuse FDG uptake in acute prostatitis. *Clin Nucl Med*. 2008;33:308–310.
9. Ho L, Quan V, Henderson R, et al. High-grade urothelial carcinoma of the prostate on FDG PET-CT. *Clin Nucl Med*. 2007;32:746–747.
10. Sexton WJ, Lance RE, Reyes AO, et al. Adult prostate sarcoma: the M. D. Anderson Cancer Center Experience. *J Urol*. 2001;166:521–525.

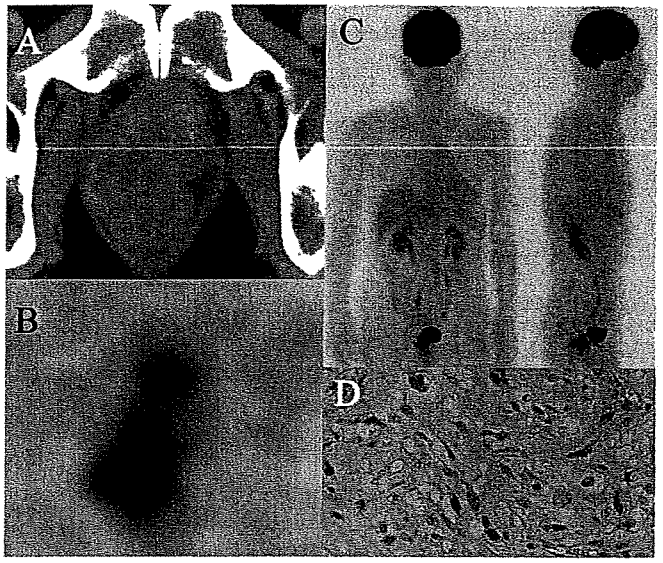

FIGURE 1. A 76-year-old man with a history of prostate cancer found to have a lobulated heterogeneous mass in the prostate gland on a follow-up pelvic computed tomography (CT). In this case, the primary prostate cancer had been treated with hormone therapy alone. Although the prostate-specific antigen (PSA) level, a marker of prostate cancer recurrence, was "undetectable" (0.3 ng/mL), the possibility of prostate cancer relapse could not be ruled out because recurrent prostate cancer has been observed in patients with low PSA levels.[1,2] The tumor was pathologically diagnosed as a prostatic sarcoma. Following this, F-18 fluorodeoxyglucose (FDG) positron emission tomography (PET) scan was performed for survey. **A,** The computed tomography scan showed a lobulated heterogeneous mass arising from the prostate gland. **B,** The transverse view of an F-18 FDG-PET scan at 60 minutes after FDG injection revealed avid-FDG uptake (maximum SUV of 7.1) corresponding to this mass. **C,** A whole body F-18 FDG-PET scan showed high FDG uptake in the prostate grand and no evidence of distant metastasis. **D,** A pathologic specimen of the prostate tumor, obtained by transperineal core needle biopsy and stained with hematoxylin and eosin, is shown. The pathologic image demonstrated overgrowth of spindle-shaped cells with hyperchromatic nuclei and frequent atypical mitosis surrounded by myxoid stroma. The tumor was immunoreactive for vimentin, P53, and ki-67, and negative for PSA. The tumor was pathologically diagnosed as a prostatic sarcoma with no evidence of existing prostatic carcinoma.

Prostatic sarcoma is extremely rare, representing only 0.1% of all prostatic neoplasms.[3] In this case, the prostatic sarcoma showed avid-FDG uptake; this has also been reported in sarcomas arising in other parts of the human body.[4,5] On the other hand, it has been reported that F-18 FDG-PET has limited value in the evaluation of prostate cancer.[6,7]

A sarcoma should be considered in the differential diagnosis, along with prostatitis and urothelial carcinoma, in cases with avid-FDG uptake on an F-18 FDG PET scan of the prostate gland.[8,9] Moreover, an F-18 FDG PET scan can be advantageous in cases of prostatic sarcoma for identifying distant metastasis, which commonly occurs and is associated with reduced survival.[10] As this case had no evidence of metastasis, intensity-modulated radiation therapy was selected for treatment.

J. Radiat. Res., 50, 281–293 (2009)

Award Review Article

Radiation-Induced Mammary Carcinogenesis in Rodent Models: What's Different from Chemical Carcinogenesis?

Tatsuhiko IMAOKA*[1], Mayumi NISHIMURA[1], Daisuke IIZUKA[1,2], Kazuhiro DAINO[1], Takashi TAKABATAKE[1], Mieko OKAMOTO[1], Shizuko KAKINUMA[1] and Yoshiya SHIMADA*[1]

Mammary/Carcinogenesis/Animal model/Chemical/Rodent.

Ionizing radiation is one of a few well-characterized etiologic factors of human breast cancer. Laboratory rodents serve as useful experimental models for investigating dose responses and mechanisms of cancer development. Using these models, a lot of information has been accumulated about mammary gland cancer, which can be induced by both chemical carcinogens and radiation. In this review, we first list some experimental rodent models of breast cancer induction. We then focus on several topics that are important in understanding the mechanisms and risk modification of breast cancer development, and compare radiation and chemical carcinogenesis models. We will focus on the pathology and natural history of cancer development in these models, genetic changes observed in induced cancers, indirect effects of carcinogens, and finally risk modification by reproductive factors and age at exposure to the carcinogens. In addition, we summarize the knowledge available on mammary stem/progenitor cells as a potential target of carcinogens. Comparison of chemical and radiation carcinogenesis models on these topics indicates certain similarities, but it also indicates clear differences in several important aspects, such as genetic alterations of induced cancers and modification of susceptibility by age and reproductive factors. Identification of the target cell type and relevant translational research for human risk management may be among the important issues that are addressed by radiation carcinogenesis models.

INTRODUCTION

Ionizing radiation is one of the few well-characterized etiologic factors of human breast cancer. Epidemiologic studies on Japanese atomic bomb survivors and on clinically irradiated patients established that female breast is among the most susceptible organs to radiation-induced cancers.[1–4)]

Animal models of radiation carcinogenesis have many advantages in providing information about radiation-associated human cancer risk. First, they are the only measure for estimating radiation-associated cancer risk when epidemiologic evidence is lacking. For example, animal experiments are essential to estimate the carcinogenic effect of neutron radiation and nuclear fuel materials.[5,6)] Second, since randomized human studies are impossible, animal experiments provide complementary information where epidemiologic studies suffer from biases and confounding factors. For instance, in the studies on Japanese atomic bomb survivors, estimation of the modifying effect of age at exposure on radiation-associated cancer risk is complicated by the chronologic changes in the background cancer incidence in some cancers; thus, cancer incidence data of the childhood exposure population are compared to the most recent incidence data, while data of the adulthood exposure group are compared to old data.[4)] Third, mechanistic understandings are essential for interpretation of epidemiologic observations, and this is provided by animal models, which are usually well defined with respect to genetic and environmental conditions.

Rodent models play an important role in understanding the natural history, mechanism, and modifying factors of breast cancer development. As discussed elsewhere,[7)] since human breast cancer is heterogeneous at the morphological, genetic and molecular levels, any given animal model could not mimic the spectrum of human breast cancers, and animal models could mimic, at best, major subsets and pathways. In

*Corresponding author: Phone: 043-206-3160,
Fax: 043-206-4138,
E-mail: t_imaoka@nirs.go.jp, y_shimad@nirs.go.jp
[1]Experimental Radiobiology for Children's Health Research Group, Research Center for Radiation Protection, National Institute of Radiological Sciences, Japan; [2]Department of Molecular Radiobiology, Research Institute for Radiation Biology and Medicine, Hiroshima University, Japan.
doi:10.1269/jrr.09027

this respect, rodent models provide a variety of breast cancer types, as reviewed below, and can be used for numerous types of studies including assays of putative oncogenic and chemopreventative agents, pathogenesis due to specific treatment regimens or genetic alterations, etc. Two classes of rodent models have been used frequently: genetically modified mouse models and chemically induced carcinogenesis models. The radiation-induced model, nevertheless, is potentially very important, since radiation exposure is one of the very few epidemiologically proven etiologic factors of human breast cancer.[7–9] As reviewed here, animal models of radiation carcinogenesis sometimes gives us observations that do not hold in other models. We focus on the difference between radiation- and chemically induced mammary carcinogenesis, with an emphasis on rat models, and attempt to clarify the future role of animal models of radiation-induced mammary cancer.

MODELS OF RADIATION-INDUCED BREAST CANCER

Reported models of radiation-induced mammary carcinogenesis in rodents are summarized in Table 1. The rat is a widely used model to study the risk and mechanism of breast carcinogenesis because rat mammary cancers are comparable to human breast cancers in many respects, such as high frequency of hormone dependence and, pathologically, progression from ductal hyperplasia and ductal carcinoma in situ.[9–11] More than fifty years have passed since induction of mammary cancer by a single X-ray irradiation of the Sprague-Dawley rat was first reported.[12] Until recently, the Sprague-Dawley rat,[13–19] as well as several Wistar-related strains (Wistar Furth, WAG, WM, and Lewis)[20–23] have been used in most studies. Although the use of other strains such as the F344 strain has been documented,[24–26] comparative studies have revealed that the Sprague-Dawley strain is most susceptible to radiation-induced mammary carcinogenesis.[26–29] The ACI rat is a unique model in which mammary cancer is induced by estrogen treatment, which can synergize with cancer induction by ionizing radiation.[30]

The mouse provides an indispensable model system in which the effects of gene manipulation can be studied in vivo. Although mouse mammary tumors do have some dissimilarities from human breast cancers, such as the low frequency of hormone dependence and the progression of carcinoma predominantly from alveolar hyperplasia,[9–11] they provide a valuable route for genetic experimentation. BALB/c mice have been used frequently in radiation carcinogenesis studies.[31] The BALB/c strain is known to harbor a unique functional polymorphism of the *Prkdc* (DNA-dependent protein kinase catalytic subunit) gene.[32] Heterozygous mutant mice of the tumor suppressor gene *Tp53*, in the genetic background of BALB/c, develop mammary cancer at a low frequency and the incidence increases after radiation exposure.[33,34] The induction is further increased by hemizygosity for *Atm*.[35] Double heterozygous mice for *Brca1* and *Tp53* also develop mammary cancer after irradiation.[36] Mutant mouse strains for *Apc* (adenomatous polyposis coli) show increased incidence of mammary tumors after irradiation, though these tumors show different histopathologic characteristics from human breast carcinoma.[37,38]

Table 1. Rodent models of radiation-induced mammary carcinogenesis

Species	Strain/genotype	Type of radiation
Rat	Sprague-Dawley	Photon, neutron, heavy ions, ^{238}Pu
	Wistar (Wistar-Furth, WAG, WM, Lewis)	Photon, neutron, ^{238}Pu
	ACI	Photon, neutron
Mouse	BALB/c	Photon, neutron
	BALB/c *Tp53*$^{+/-}$	Photon
	BALB/c *Tp53*$^{+/-}$ *Atm*$^{+/-}$	Photon
	Brca1$^{+/-}$ *Tp53*$^{+/-}$ (strain unspecified)	Photon
	C57BL/6 *Apc*$^{Min/+}$, *Apc*$^{1638N/+}$	Photon

In addition to sparsely ionizing (low linear energy transfer [LET]) radiations such as photon (X- and γ-ray) radiation, induction of mammary cancers is observed after administration of densely ionizing (high LET) particle radiations including neutrons and heavy ions. Rat and mouse models have provided important information on the risk of neutrons[5,39–41] and heavy ion radiations including neon, iron, and carbon ions.[29,42,43] These studies have indicated the high relative biologic effectiveness of high-LET radiation for mammary cancer induction. Mammary cancer development following administration of plutonium has also been documented.[44]

To briefly summarize chemically induced mammary carcinogenesis models, BALB/c, FVB, and other strains of mice are frequently used for mammary cancer induction by two classes of carcinogens: polyaromatic hydrocarbons (methylcholanthrene, 1,2:5,6-dibenzanthracene, and 7,12-dimethylbenz(a)anthracene [DMBA]) and alkylating agents (1-methyl-1-nitrosourea [MNU], 1-ethyl-1-nitrosourea [ENU], and urethane).[8] Rat mammary cancers are usually induced by a single, high-dosage treatment with DMBA or MNU.[45] Also used recently is a protocol in which rats are treated repeatedly with heterocyclic amines such as 2-amino-1-methyl-6-phenylimidazo[4,5-*b*]pyridine (PhIP), a representative food-borne carcinogen.[46] Sprague-Dawley and F344 rats are among the most frequently used rat strains in these studies.

PATHOLOGY AND NATURAL HISTORY

Extensive descriptions of the pathology of radiation- and chemically induced rodent mammary tumors have been documented in several excellent reviews.[45,47,48] Very briefly, development of benign mammary tumors such as fibroadenoma is prominent after irradiation of rats, although significant development of adenocarcinoma (malignant tumor) is observed.[49] In comparison, chemical carcinogens tend to induce mainly adenocarcinoma.[45] To date, no pathologic differences between chemically induced and radiation-induced adenocarcinomas have been documented.[45]

Temporal histopathologic changes leading to the development of carcinoma in the chemical carcinogenesis model have been extensively studied.[9] The mammary gland consists of epithelial tissue of the mammary ducts embedded in fatty stromal tissue (Fig. 1A). In the course of normal organogenesis, the mammary gland rapidly grows during and after puberty, when mammary ducts elongate and bifurcate to fill the subcutaneous mammary fat pad (Fig. 1B). This is achieved by a controlled balance of cell proliferation and death within the terminal end bud (TEB), the club-shaped structure at the growing ductal terminus, which is present from prepubertal to postpubertal stages (Fig. 1C).[50] Differentiated structures such as terminal ducts and alveolar buds are formed along the duct (Fig. 1C) and, as the gland attains full development, TEBs also regress and differentiate into one of these structures.[51] Many lines of evidence suggest that the TEB is the major target structure of chemical carcinogens. After treatment of rats with chemical carcinogens, TEBs show pathological changes such as delayed regression, high proliferation index, and consequent development of hyperplastic and premalignant ductal lesions.[52–54]

Information regarding radiation-induced carcinogenesis is relatively limited. In mice and rats, pyknotic nuclear aberration and suppressed cell proliferation have been observed in TEBs at 6–24 hours after irradiation, which return to normal levels by 1.5–3 days.[55,56] Delayed regression of TEBs, with sustained cell proliferation, and development of ductal hyperplasia are seen 4–8 weeks after irradiation of rats (Fig. 2).[55] These changes are similar to those observed after stimulation with chemical carcinogens, as mentioned above. Hyperplastic alveolar nodules (HANs) are induced by X-irradiation in rats,[57] though they are not considered to be precursor lesions of rat mammary carcinoma in chemical induction models.[9] Thus, evidence suggests that the pathogenesis of radiation-induced mammary carcinogenesis may be largely similar to that of chemical carcinogenesis.

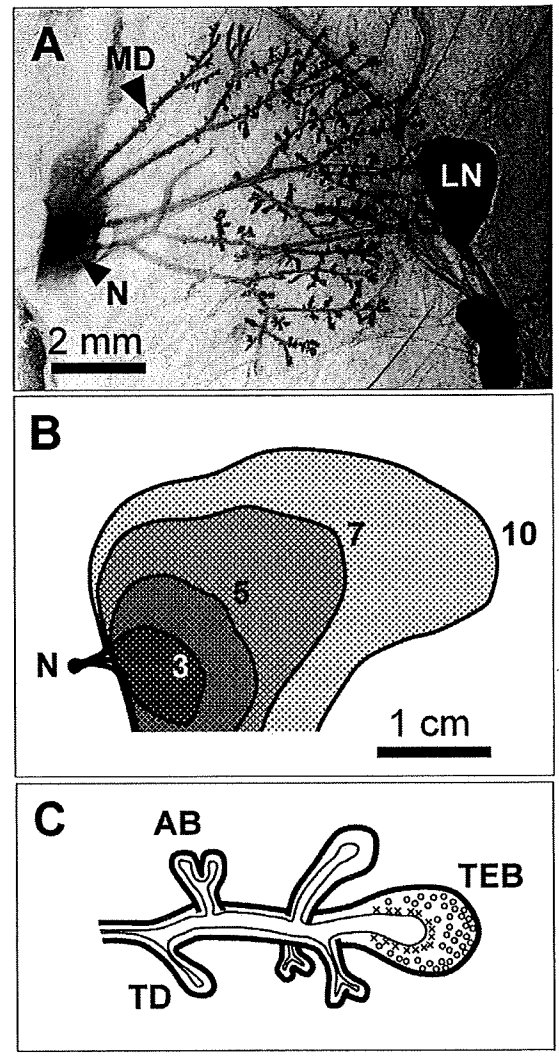

Fig. 1 Normal mammary gland development in the rat. (A) A photomicrograph of a whole-mount preparation of the rat mammary gland at 3 weeks of age. *LN*, lymph node; *MD*, mammary duct; *N*, nipple. (B) A schematic drawing depicting the area occupied by the mammary epithelial tissue during pre- and postpubertal development in the rat. Numbers indicate age in weeks. (C) A schematic illustration of structures of the mammary epithelial tissue around the postpubertal period. *AB*, alveolar bud; *TD*, terminal duct; *TEB*, terminal end bud. Regions of proliferating (*circles*) and apoptotic cells (*crosses*) in TEB are indicated.

GENETIC CHANGES IN CANCER

One characteristic property of ionizing radiation is that it produces DNA double strand breaks, in addition to other oxidative damage; as a consequence, deletions and discontinuous loss of heterozygosity (LOH) are a signature of the mutagenic action of radiation.[58] On the other hand, carcinogenic chemicals used to induce mammary cancer generally generate adducts to DNA and result in base substitutions and small deletions.[59]

Base substitution mutations (especially at codons 12 and 13) in the H-*ras* proto-oncogene are frequently seen in

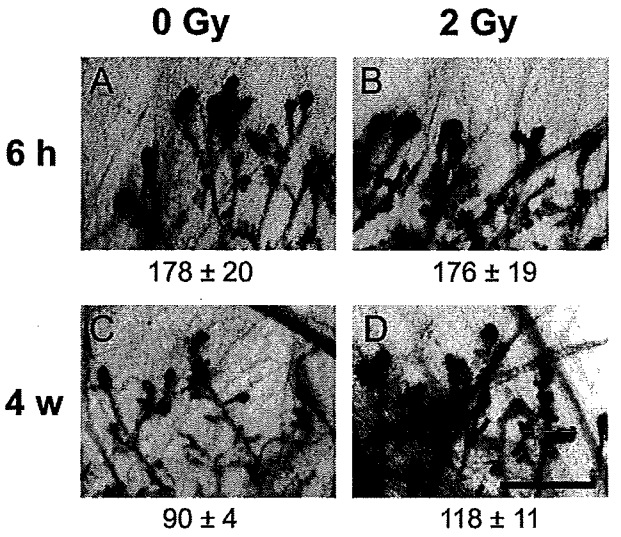

Fig. 2. Delayed regression of the terminal end bud (TEB) after irradiation. Rats were either untreated (*0 Gy*) or X-irradiated (*2 Gy*) at 7 weeks of age and whole-mount preparations of the mammary gland were prepared at 6 hours (*upper panels*) and 4 weeks (*lower panels*) after irradiation. *Bar*, 1 mm. Numbers below each panel indicate mean diameters of TEBs (μm; mean ± S.D., $n = 3$). Modified based on the data in Imaoka *et al.*[55]

MNU-induced rat mammary cancer[60] and to a lesser extent in PhIP-induced ones[61–63] but not in DMBA-induced cancers.[64] Rat mammary cancers induced by γ-rays and heavy ions harbor no mutation of H-*ras*,[29,65] as expected from their preferential induction of deletions and LOH. H-*ras* mutation is thus unlikely to be a causative event in radiation-induced rat mammary carcinogenesis.

LOH is one of the mechanisms through which tumor suppressor genes are inactivated in cancer cells. Searching for LOH regions in cancer, therefore, is generally a promising strategy to discover important tumor suppressor genes. Several LOH regions have been found in PhIP-induced rat mammary cancers,[66,67] whereas LOH is a rare event in DMBA-, MNU-, and radiation-induced rat mammary cancers.[20,68] The low frequency of LOH in radiation-induced mammary cancer is surprising considering the ability of ionizing radiation to induce LOH in other studies.[58,69,70] Comparative genomic hybridization is a powerful tool to detect amplification and deletion of chromosomal regions and has been used to study PhIP- and DMBA-induced rat mammary cancers.[71] This analysis has revealed that amplification of several chromosomal regions is characteristic to PhIP-induced cancer, whereas such copy number aberrations are absent in DMBA-induced cancers.[71] Studies on radiation-induced cancer are awaited.

Comprehensive gene expression profiling using microarrays is a warranted strategy to dissect important gene expression changes. Rat mammary cancers induced by ionizing radiation, PhIP, DMBA, MNU, and other chemical carcinogens, as well as spontaneously arising mammary cancers, have been analyzed in this manner.[72–77] Many of these studies have questioned if cancers of different etiological origins exhibit different gene expression patterns. The results indicate the existence of some differences in gene expression patterns; however, the expression of most genes seems to be similar between cancers of different etiological origins.

Epigenetic events such as alteration of DNA methylation at CpG islands have not been extensively studied in rodent mammary cancer models, and remain an open and promising area of research. Taken together, evidence so far suggests that the genetic alterations may be different between radiation and chemical carcinogenesis models, but the resulting alterations in gene expression are largely similar.

INDIRECT EFFECTS OF CARCINOGENS

Although direct genetic alteration is believed to be the principal role of ionizing radiation in carcinogenesis, evidence suggests the existence of some other effects. An in vitro study has suggested the effect of irradiated human mammary fibroblasts on co-cultured non-irradiated mammary epithelial cells to disrupt normal morphogenesis of epithelial ducts.[78] An in vivo study has revealed that irradiated mouse mammary stroma has the ability to transform a non-tumorigenic mammary cell line to a tumorigenic state upon transplantation of the cells into stroma.[79] Stroma-derived transforming growth factor β (TGFβ) may be involved in mediating such indirect effects of ionizing radiation. Evidence indicates that irradiation induces chronic activation of TGFβ in the fatty stroma of the mouse mammary gland,[80,81] and may cause remodeling of the stromal extracellular matrix.[81] Activated TGFβ may also translocate to the epithelial tissue[80,81] and mediate p53-dependent radiation response and epithelial-mesenchymal transition.[82,83] In chemical carcinogenesis, a similar indirect (stroma-mediated) effect of MNU has been documented in a rat experiment in which non-treated mammary epithelium gives rise to cancer after being transplanted into the mammary stromal fat of MNU-treated rats.[84] In contrast, the stroma is not a major target in DMBA-mediated tumorigenesis of mouse mammary preneoplastic cells.[85] These opposing lines of evidence may indicate differences in the mode of action of the carcinogens, differences between species (mouse vs. rat), or differences in experimental design. Because more information is currently available for radiation carcinogenesis models, future comparative studies using chemical induction models could offer important clues to unveiling a more complete picture of such indirect carcinogenic effects.

RISK MODIFICATION BY REPRODUCTIVE FACTORS

Human breast cancer risk is positively associated with obesity (high body mass index) as well as reproduction-related risk factors such as early age at menarche, late age at first full-term pregnancy, and late age at menopause, all of which are related to a prolonged period of endogenous estrogen exposure.[86] A study of atomic bomb survivors indicated that many of these factors, as well as estrogen use, modify the radiation-associated risk of breast cancer in women.[87] Estrogen-related modification of mammary cancer induction is thus an important issue in animal models.

Estrogen receptor (ER) expression of tumors is associated with the estrogen responsiveness of tumors. Whereas non-ovariectomized rats develop ER-positive mammary cancers after irradiation, prepubertally ovariectomized rats, irradiated at adulthood, develop ER-negative mammary cancer, albeit at a low incidence.[88,89] Similarly, most mammary carcinomas that develop in prepubertally MNU-treated rats are ER-positive, whereas ER-negative carcinoma develops at a low incidence when the rats are ovariectomized shortly after MNU treatment.[90,91] Most DMBA-, MNU-, and radiation-induced rat mammary cancers undergo regression after ovariectomy and are thus ovary dependent.[92–94] These results are consistent in that the estrogen/ER signaling plays pivotal roles in promotion/progression and maintenance of most radiation- and chemically induced rat mammary cancers.

Regarding the risk modification by parity, pregnancy reduces the incidence of chemically induced rat mammary cancer whether carcinogen is administered before, during, or after pregnancy.[95–97] This protective effect of parity may be due to pregnancy-associated changes in the systemic hormonal environment,[98,99] the mammary gland content of hormone-responsive cells,[95] and the initial responsiveness of the mammary cells to carcinogens.[100,101] In contrast, pregnancy after irradiation does not affect the incidence of rat mammary cancer.[102] The incidence of mammary cancer in rats irradiated during pregnancy, lactating, or post-lactating stages is no different from that in age-matched virgins.[103] When virgin, pregnant, and lactating rats are irradiated and then subjected to long-term estrogen treatment (*i.e.*, identical promotional environment), the lactating rat is by far the most susceptible, while the virgin is most resistant.[104] Further studies such as transplantation experiments may be needed to distinguish between these putative initiation- and hormone-related effects of parity on radiation carcinogenesis.

RISK MODIFICATION BY AGE AT EXPOSURE

One important issue in risk assessment of carcinogens is the modifying effect of age at time of exposure. A surprisingly high incidence of early-onset breast cancer is observed in atomic bomb survivors who were exposed in childhood.[105,106] Several studies have addressed this issue using both rat and *Apc*$^{Min/+}$ mouse models of radiation-induced mammary carcinogenesis.[21,27,38,94] Though the mechanism is not understood, the carcinogenic effect of prepubertal radiation exposure is small, the effects of postpubertal and adulthood exposures are larger, and the effect in old (> 60 weeks) animals is low (Fig. 3A).[21,27,38,94] This pattern is different from the narrow window of the susceptible period in chemically induced rat mammary carcinogenesis (Fig. 3B). Since the high susceptibility of postpubertal rats to DMBA does not exactly coincide with the number of TEBs or their proliferation index, this window of susceptibility is understood in association with the transitional differentiation state of TEBs into alveolar buds around this age.[107] In addition, the low level of DMBA-DNA adducts in prepubertal rats[108] may

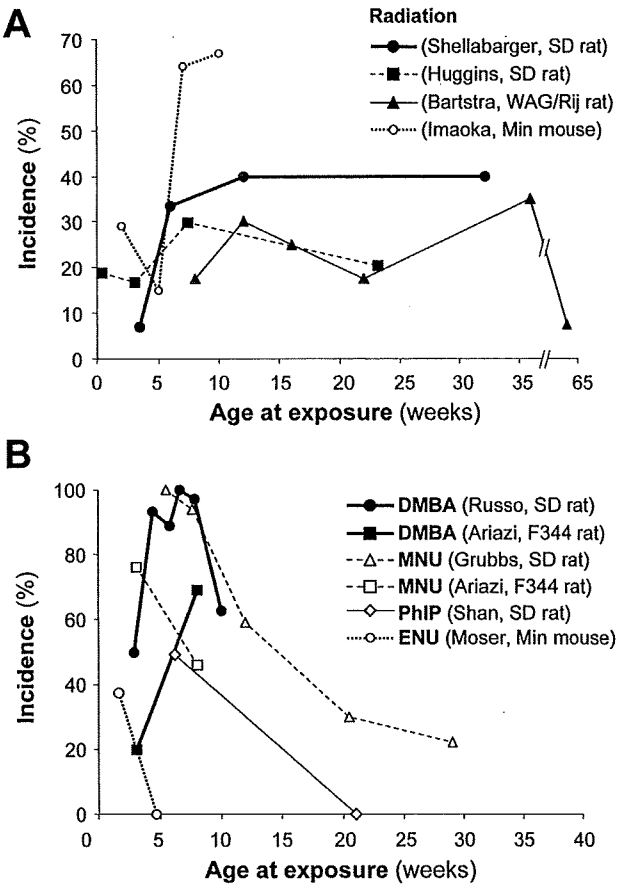

Fig. 3. Dependence on age at exposure of mammary tumor induction with ionizing radiation and chemical carcinogens in rodent models. (A) Radiation carcinogenesis data from literature.[21,27,38,94] (B) Chemical carcinogenesis data from literature.[107,109,110,112,113]

indicate weak metabolic activation of DMBA into its carcinogenic form in immature mammary gland. Administration of MNU to prepubertal rats is more effective in inducing mammary cancer than that to postpubertal rats, and the susceptibility decreases with age thereafter (Fig. 3B).[109,110] This age dependence of MNU is explained by deficiency of a DNA repair enzyme in immature rat mammary epithelial cells.[111] A similar age dependence is observed for ENU-induced mammary carcinogenesis of *Apc*$^{Min/+}$ mice (Fig. 3B).[112] The carcinogenic effect of PhIP is higher in pubertal rats than in mature animals (Fig. 3B).[113] This modifying effect of age does not correlate with either PhIP-DNA adduct levels or PhIP-induced mutation frequency, but is only explained by age-dependent gene expression changes induced by PhIP administration.[113] These studies suggest that, in mammary cancer induction, the modifying effect of age at exposure and its underlying mechanism are largely dependent on the carcinogen species.

MAMMARY TARGET CELLS OF CARCINOGENS

The mammary epithelium contains small fractions of stem cells (which are able to reconstitute the whole gland) and progenitor cells (with partial regenerative potency) plus a large population of differentiated cells.[114,115] The existence of mammary stem cells was first suggested by the complete regeneration of mammary gland after inoculation of isolated mammary epithelial cells into subcutaneous fat pads of syngeneic mice.[116] The regenerative activity of the rat mammary stem/progenitor cells is measured by inoculating dispersed mammary epithelial cells into the mammary fat pad of other rats and analyzing any resulting formation of colonies.[114] The unit of colony formation therein is termed a clonogen and is thought to represent individual stem and/or progenitor cells. In fact, these colonies contain cells that produce morphologically different (i.e., ductal and alveolar) colonies upon subsequent transplantation, indicating the stem cell–like property of clonogenic cells.[117] A significant number of clonogens survive after irradiation at a carcinogenic dose, and cancer initiation is calculated to occur frequently in surviving clonogens.[118–120] These observations suggest that mammary stem/progenitor cells that survive radiation exposure may initiate cancer development. Indeed, recent studies have identified a population of mouse mammary stem cells (CD49f^{high}/CD24^{med} or CD29^{high}/CD24^{+})[121,122] that are sensitive to a high dose (4 Gy) of radiation,[123] whereas a putative progenitor cell population (CD29^{-}/CD24^{-}/Sca-1^{high}) is radioresistant and enriched 24 hours after irradiation.[123]

The generative feature of the TEB, producing all mammary epithelial structures, strongly suggests the existence of stem cells in the TEB; however, the fact that transplantation of any portion of the gland parenchyma generates a complete gland also indicates their existence throughout the gland.[124] As mentioned above, mammary carcinogenesis induced by acute postpubertal stimulation is likely to originate mainly from TEBs. Because the TEB consists of proliferating, undifferentiated cells,[50] the target cell type of carcinogens may be stem or progenitor cells, which are abundant in this structure. However, since TEBs disappear once the postpubertal mammary gland development is complete, they do not seem to be important in spontaneous mammary cancer development in non-treated animals or in cancer induction by long-term or adulthood carcinogenic treatment. A careful observation of MNU-induced premalignant lesions that are disseminated throughout the gland[9] also implies that some cells outside TEBs are involved in cancer initiation.

Cancer development in humans may be a result of accumulation of mutations over a long period of time. This assumption strongly suggests that the tissue stem/progenitor cell, which has a long lifespan, is the cell type from which cancer arises. Detection of long-term label-retaining cells is one criterion to indicate the existence of long-lived cells in vivo. In the mouse mammary gland, radiolabeled thymidine, administered to virgin mice, is retained in a subset of cells for more than 6 weeks (even after pregnancy).[125–127] A double-labeling experiment has suggested that the radiolabeled DNA molecules are retained in the cells through preferential retention of the template DNA strands within the long-lived mother cells during chromosomal segregation.[125] Long-lived (9 weeks), label-retaining cells of the mouse mammary gland contain enriched Sca-1^{+} cells, a putative progenitor cell population.[128] In experimental carcinogenesis, fractionation and protraction of irradiation is a unique method to induce mutations selectively in long-lived cells. Protracted irradiation over a period of 16–28 weeks is known to induce rat mammary cancer at a level comparable to that after a single irradiation at the same total dose.[129,130] This observation indicates that the long-lived cell population is an important target cell type in radiation carcinogenesis, even if one takes into account the repair of damage after each fractionated irradiation.

In the rat model of mammary cancer induction by a single postpubertal irradiation, a short-term estrogen treatment during a period around irradiation increases the incidence of mammary cancer in rats[24,28,131] and treatment with an ER antagonist reduces the incidence.[15] Incidence of radiation-induced rat mammary cancer is also decreased by temporary hormonal ablation by ovariectomy prior to irradiation, followed by chronic estrogen supplementation after irradiation.[88,89] This reduction is recovered by estrogen treatment immediately after ovariectomy, but not by progesterone or prolactin. These lines of evidence suggest the involvement of estrogen-responsive cells in cancer initiation. Interestingly, in rats treated chronically with estrogen, protraction of irradiation over a period greater than 8 weeks diminishes the radiation-associated mammary cancer risk that is otherwise evident at the same total dose.[130] This estrogen-dependent protraction effect is explained by damage repair

in estrogen-responsive cells or, more attractively, the high susceptibility of estrogen-responsive target cells with a lifespan less than 8 weeks. Indeed, steroid hormone receptor expression is absent in mouse mammary stem cells isolated by surface markers and in long-lived (9 weeks) label-retaining cells,[128,132,133] whereas ER-expressing cells are enriched in label-retaining (7 weeks) cells of estrogen-stimulated mice.[126]

Taken together, it is postulated that, upon acute high-dose irradiation, most mammary stem cells may be killed and progenitor cells with induced mutations may proliferate thereafter. These progenitor cells may have a long life (in nature or by taking the evacuated stem cell niche), accumulate further mutations, and finally give rise to cancer. During repeated low-dose exposures, both stem and progenitor cells may survive and accumulate mutations. Estrogen may increase the number of estrogen-responsive progenitor cells that can be targeted by carcinogens. This working hypothesis must be challenged by further investigation. Identification of the target cell type has an important meaning for risk assessment, in that an infinite lifespan of the target cell would permit accumulation of mutations over the life time of the individual, and necessitate long-term management of exposure history.

PERSPECTIVE AND CONCLUSION

Animal models of radiation carcinogenesis are valuable tools to study underlying mechanisms of relevant human carcinogenesis. Among recent progresses in breast cancer research is the finding that human breast cancers are subdivided into the following five subtypes based on characteristic gene expression: luminal A, luminal B, HER2 (human epidermal growth factor receptor 2)–positive, normal-like, and basal-like.[134] Human breast cancer of the basal-like subtype shows triple negativity for ER, progesterone receptor, and HER2, but is positive for expression of basal markers such as cytokeratin 5/6.[134] It is noteworthy that mammary gland stem cells of mice show basal-like phenotypes.[132] Also interesting is the observation that many of the human breast cancers that develop after radiation therapy are associated with basal-like phenotypes.[135] Recently established mouse models of basal-like breast cancer[136–138] and yet-to-be-established carcinogenic induction models of these subtypes would provide valuable information on the mechanism underlying development of carcinogen-induced breast cancer and the relevance of the stem cell population as a target of carcinogens.

The evidence reviewed herein indicates that radiation and chemical carcinogenesis models of mammary cancer share certain characteristics, although some differences do exist (Table 2). TEB may be the major origin of premalignant lesions that progress into cancer in both radiation and chemical models, at least after postpubertal acute carcinogenic stimulation. The cancers in these models exhibit mostly similar gene expression profiles, albeit with some differences,

Table 2. Comparison of radiation and chemical models of mammary carcinogenesis*

Feature	Radiation	Chemical
Epidemiology	Abundant	Scarce
Pathology	Adenocarcinoma, fibroadenoma	Mainly adenocarcinoma
Genetic changes		
H-*ras* mutation	No	Yes (MNU, PhIP); no (DMBA)
LOH	Rare	Frequent (PhIP); rare (DMBA, MNU)
Transcriptome	Changed	Changed
Indirect effect	Possible	Possible
Risk modification		
Estrogen	Increases risk	Increases risk
Parity	Not protective	Protective
Susceptible age	Postpubertal	Postpubertal (DMBA); prepubertal (MNU); pubertal (PhIP)
Target structure	TEB, non-TEB	TEB (DMBA, MNU), non-TEB (MNU)

* Abbreviations. DMBA, 7,12-dimethylbenz(a)anthracene; LOH, loss of heterozygosity; MNU, 1-methyl-1-nitrosourea; PhIP, 2-amino-1-methyl-6-phenylimidazo[4,5-b]pyridine; TEB, terminal end bud.